Modeling CCN activity of chemically unresolved model-HULIS, including composition-dependent surface tension, non-ideality, and surface partitioning

Nønne L. Prisle[1,2] and Bjarke Mølgaard[2]

[1]University of Oulu, Nano and Molecular Systems Research Unit, P.O. Box 3000, 90014, University of Oulu, Finland
[2]University of Helsinki, Department of Physics, P.O. Box 48, 00014, University of Helsinki, Finland

Correspondence: N. L. Prisle
(nonne.prisle@oulu.fi)

Abstract. We present a thermodynamically consistent model that enables self-contained, predictive calculations of droplet growth and activation with considerations of surface adsorption, surface tension reduction, and non-ideal water activity for chemically unresolved, complex surface active aerosol mixtures. The common presence of surface active organic material in atmospheric aerosols is now well-established, whereas the influence of surface activity on aerosol hygroscopic growth and cloud droplet activation remains to be fully constrained. Because specific characterization of key properties, such as water activity and surface tension, are challenging to obtain directly for finite-sized activating droplets, a robust model framework is needed to gain further insight into the droplet equilibrium growth process. The present model is based on coupling Köhler theory with the Gibbs adsorption and Szyszkowski-type surface tension equations and formulated on a mass-basis to allow for a quantitative description of chemically unresolved mixtures. The model is used to calculate cloud condensation nuclei (CCN) activity of aerosol particles comprising Nordic Aquatic Fulvic Acid (NAFA), a surface active model atmospheric humic-like substance (HULIS), and NaCl with dry diameters of 30–230 nm and compositions spanning the full range of relative NAFA and NaCl mixing ratios. Parametrizations of aqueous surface tension and water activity with respect to independently varying NAFA and NaCl mass concentrations were developed to obtain continuous descriptions of non-ideal interactions governing both bulk and surface properties during droplet growth and activation. Effects of NAFA surface activity are gauged *via* a suite of properties evaluated for growing and activating droplets and results are compared to those of several other predictive Köhler frameworks, where surface active components in droplet solutions are considered in different ways. Failing to account for bulk/surface partitioning of NAFA introduces severe biases in evaluated droplet bulk and surface compositions, which here specifically affect Köhler activation thermodynamics, but more generally could also impact heterogeneous chemistry on droplet surfaces. Simpler models based on approximating surfactant partitioning and/or neglecting surface tension reduction give similar results as the comprehensive partitioning model and reproduce previously reported experimental CCN activity well, reflecting how the finite amounts of surface active material in microscopic droplets are strongly depleted from the bulk phase due to bulk/surface partitioning because surface areas for a given bulk volume are very large. As a result, both evaluated surfactant strength and hygroscopicity of NAFA is significantly lower in finite-sized activating droplets than in macroscopic aqueous solutions of the same overall composition.

1 Introduction

The surface activity of atmospheric aerosol components and its implications for cloud microphysics have been investigated for several decades. By definition, surface active (surfactant) material adsorb at the surface of a solution, leading to enhanced surface concentrations (activity), compared to the (interior) bulk, and a resulting radial concentration gradient between the surface and bulk phases. Due to this enhanced surface activity, surfactants can typically reduce surface tension of aqueous solutions more efficiently at a given concentration than homogeneously mixed solutes. Shulman et al. (1996) showed that reduced surface tension in aqueous droplets can alter the shape of their equilibrium growth curve as described by Köhler theory (Köhler, 1936) and thereby lower the critical supersaturation threshold for cloud droplet activation. Facchini et al. (1999, 2000) then demonstrated that surface active material is indeed present in atmospheric cloud and fog samples, which can significantly reduce aqueous surface tension at concentrations comparable to those of activating droplets. Surface active components have now been found in aerosols from many different environments (e.g. Petters and Petters, 2016; Gérard et al., 2016; Kroflič et al., 2018).

Köhler calculations generally require composition-dependent droplet properties in some form. The surface equation-of-state for a solution can be given in terms of either the surface or bulk composition, as these quantities are related *via* the equilibrium bulk-to-surface concentration gradient for a given surface active substance. A number of techniques exist to experimentally determine the surface tension–composition relations for surfactant solutions, which almost exclusively require macroscopic (i.e. millimeter-scale or larger) sample sizes (Fainerman et al., 2002; Hyvärinen et al., 2006; Kristensen et al., 2014; Bzdek et al., 2020). In these macroscopic solutions, surface adsorption and enhanced surface activity involve only a small fraction of the total amount of surface active solute and therefore have negligible effect on the bulk composition. As a consequence, surface tension–composition relations reported in terms of total solute concentrations, which are readily quantified experimentally for macroscopic solutions, closely reflect the corresponding bulk composition.

For finite-sized solutions, such as microscopic and sub-micron activating cloud droplets, surface adsorption can significantly deplete the bulk-phase of surface active solute, because the total amount of solute in the system is finite, and the surface area (A) to bulk volume (V) ratio may be several orders of magnitude greater than for macroscopic solutions (Prisle et al., 2010; Lin et al., 2020): For a spherical system, where the diameter d represents the characteristic dimension, $A/V = 6/d = 6\times10^6$ m^{-1} for a 1 μm droplet and $A/V = 6000$ m^{-1} for a macroscopic droplet with $d =$1 mm. The highly sensitive variation of A/V with finite solution size introduces a size-dependent shift in both surface and bulk concentrations at the adsorption equilibrium of the surface active species.

The distribution of surface active species between the distinct bulk and surface phases of a solution is referred to as the bulk/surface *partitioning*. Size-dependent partitioning has been predicted to in turn result in size-modulated composition-dependent properties for finite-sized solution droplets (Bianco and Marmur, 1992; Laaksonen, 1993; Sorjamaa et al., 2004; Prisle et al., 2010), including surface tension (a surface property) and water activity (a bulk property), which are key parameters in determining aerosol water uptake, hygroscopic growth and cloud droplet activation. Until recently, experimental evidence for this effect in cloud microphysics has been indirect, from the reported inability of Köhler models using macroscopic solution property–composition relations to reproduce observed droplet activation. For example, a range of studies have consistently demonstrated that using surface tension and water activity relations based on total solution composition, without explicit consideration of the impact of surface adsorption on bulk composition, can lead to dramatic over-estimations of cloud condensation nuclei (CCN) activity (Li et al., 1998; Sorjamaa et al., 2004; Prisle et al., 2008, 2010; Kristensen et al., 2014; Hansen et al., 2015; Petters and Petters, 2016; Lin et al., 2018; Forestieri et al., 2018; Prisle et al., 2019). Recently, Bzdek et al. (2020) presented the first measurements of concentration dependent surface tensions for finite-sized, surfactant-containing aqueous droplets and provided the first direct experimental evidence for the influence of bulk-phase depletion from size-dependent bulk/surface partitioning.

Effects of surfactant bulk/surface partitioning may greatly impact predictions of the cloud forming potential of surface active aerosol (Laaksonen, 1993; Li et al., 1998; Sorjamaa et al., 2004). In Köhler calculations, macroscopic solution property–composition relations are connected to those of growing droplets with changing A/V *via* a partitioning model, which is typically based on a suitable adsorption isotherm and surface tension equation of state for the surface active components. An overview of the most widely used partitioning models in Köhler modeling is given by Malila and Prisle (2018). Thermodynamic process models, such as those presented by Prisle et al. (2010), Topping (2010), Raatikainen and Laaksonen (2011), Petters and Kreidenweis (2013) and Malila and Prisle (2018), generally rely on input of compound-specific properties with well-characterized composition dependencies. Due to the challenges involved in obtaining sufficient amounts of atmospheric samples and characterizing their composition and composition-dependent properties in aqueous solution, including surface activity (e.g. Kroflič et al., 2018; Prisle et al., 2019), many process-level experimental and modeling studies have used sodium dodecyl sulfate (SDS) and similar industrial surfactants with relatively well-known properties as model compounds for surface active components of real atmospheric aerosols (e.g. Li et al., 1998; Sorjamaa et al., 2004; Harmon et al., 2010; Prisle et al., 2011; Raatikainen and Laaksonen, 2011; Petters and Kreidenweis, 2013).

The first atmospheric surfactants used in Köhler calculations together with a thermodynamic partitioning model were straight-chain fatty acid sodium salts (Prisle et al., 2008, 2010, 2011; Forestieri et al., 2018), which are widely identified in atmospheric aerosol samples (e.g. Yassaa et al., 2001; Mochida et al., 2002, 2003; Cheng et al., 2004). Both SDS, fatty acids, and their salts are relatively strong surfactants (Prisle et al., 2008, 2010, and references therein), yet the modeled effect of surface tension on CCN activation was very modest, due to strong depletion of the surfactant molecules from the bulk phase in activating droplets arising from surface partitioning. Overall, these model predictions reproduced experimental observations of CCN activity well. The atmospherically relevant surfactants so far studied in terms of detailed compound-specific solution properties (see e.g. overview by Petters and Petters, 2016) comprise a relatively narrow selection of often simple, homologous molecules, which most likely do not represent the properties of all atmospheric surface active compounds. Furthermore, the binary and ternary aqueous droplet mixtures which are typically the focus of process-level studies may constitute too simple proxy systems to capture the variation of properties displayed by chemically complex surface active aerosol mixtures in the atmosphere. Significant variation in aerosol surface activity may be reflected in the somewhat diverging messages regarding the importance of surface tension for closure of CCN number concentrations from different studies (e.g. Wex et al., 2007; Varga et al., 2007; Asa-Awuku et al., 2008; Booth et al., 2009; Poulain et al., 2010; Frosch et al., 2011; Ovadnevaite et al., 2017).

Atmospheric aerosol samples, as well as those generated in more elaborate laboratory experiments, often comprise complex mixtures which are chemically either partially or entirely unresolved. A major challenge in establishing general results for the role of surface active aerosol in cloud microphysics relates to the composition-dependent thermodynamic description and process modeling of such chemically diverse and unresolved aerosol mixtures. Even in the hypothetical case where all aerosol components and their quantities would be known, it is often not realistic to obtain a well-constrained description of their interactions in all solution states corresponding to growing droplets. To enable thermodynamic calculations, one approach is to assume a well-known proxy compound or mixture to represent the properties of the complex system. A key challenge of this approach concerns how representative the chosen proxy is of the actual aerosol mixture and in particular how well it represents the response of the mixture to varying conditions. Furthermore, for all but a relatively small group of atmospherically relevant compounds, interaction parameters even for binary, as well as higher order, aqueous solutions are typically not constrained by measurements. Alternatively, Prisle et al. (2011) proposed a very simple framework for representing the overall effect of aerosol surface activity on CCN activation. This model rather crudely assumes that surface active components are completely partitioned to the droplet surface with a resulting effective hygroscopicity parameter of $\kappa = 0$ (Petters and Kreidenweis, 2007) and vanishing impact on droplets surface tension. The simple representation was demonstrated to perform well for SDS and fatty acid salts with 8–12 carbon atoms ($\mathrm{C_8, C_{10}, C_{12}}$), the activation behavior of which it was first proposed to emulate, but a more general applicability still remains to be established.

Here, we present a framework that enables predictive, thermodynamically consistent calculations of droplet growth and activation for chemically unresolved, complex surface active aerosol mixtures. Following the approach of Prisle et al. (2010), Köhler theory is coupled with a partitioning model based on the Gibbs adsorption and Szyszkowski-type surface tension equations. To allow for a quantitative description of chemically unresolved components, the model is formulated on a mass-basis and continuous parametrizations for bulk water activity and surface tension in aqueous solutions are constructed from macroscopic measurements, where composition-dependency is described in terms of mass-concentrations without specific knowledge of the molecular identity of all solution components.

The model is applied to evaluate a suite of properties, including critical supersaturation and droplet size, bulk-phase composition, water activity, surface tension and Kelvin effect, for growing and activating droplets formed from particles comprising Nordic Aquatic Fulic Acid (NAFA) mixed with sodium chloride (NaCl). NAFA is one of several commercial reference compounds used as models for atmospheric HUmic LIke Substances (HULIS), which comprise another major group of atmospheric surface active organics (e.g. Kiss et al., 2005; Dinar et al., 2006b; Graber and Rudich, 2006). Kristensen et al. (2014) and Lin et al. (2020) report a comprehensive data set, including measurements of CCN activity for particles with a range of sizes comprising NAFA and NaCl in various mixing ratios, as well as surface tension and water activity of macroscopic aqueous NAFA–NaCl solutions. NAFA significantly reduces surface tension in macroscopic aqueous solutions, similar to other model HULIS (e.g. Kiss et al., 2005; Aumann et al., 1967). However, Kristensen et al. (2014) found that CCN activity of both pure NAFA and mixed NAFA–NaCl particles was significantly overestimated by Köhler calculations assuming the impact of NAFA surface activity on droplet surface tension to be equivalent to that measured in the corresponding macroscopic solutions. This strongly suggests that size-dependent bulk/surface partitioning of NAFA in microscopic droplets also needs to be taken into account to explain the observed CCN activity. The predictive thermodynamic framework provides a means to gain insight into the detailed process-level mechanisms governing the particle size and composition dependent variations in CCN activity of chemically complex, unresolved surface active NAFA aerosol mixtures.

2 Theory and modeling

CCN activity for NAFA particles of varying dry sizes and mixing ratios with NaCl salt was calculated using a framework based on the Köhler equation (Köhler, 1936; Prisle et al., 2010) in the form

$$\frac{SS}{[100\%]} \equiv \frac{p_{\mathrm{w}}}{p_{\mathrm{w}}^{0}} - 1 = a_{\mathrm{w}} \exp\left(\frac{4\sigma\nu_{\mathrm{w}}}{RTd}\right) - 1\,. \tag{1}$$

Equation 1 describes the equilibrium water vapor supersaturation (SS) over a spherical solution droplet as a function of its diameter (d): p_{w} is the equilibrium partial pressure of water over the solution droplet, p_{w}^{0} is the saturation vapor pressure over a planar surface of pure water, a_{w} and σ are the water activity and surface tension of the droplet solution, ν_{w} is the partial molar volume of water in solution, approximated as the ratio of pure water molar mass and mass density $M_{\mathrm{w}}/\rho_{\mathrm{w}}$, R is the universal gas constant, and T is the Kelvin temperature. The solution droplet is formed as water condenses onto an initially dry particle. Only the dry particle before any water uptake has occurred is here referred to as a "particle" and dry particle diameters (as well as other properties) are designated in upper case symbols, as D_{p}. After water uptake, the wet aerosol particle is referred to as a (solution) droplet, and corresponding diameters (and other properties) are designated in lower case symbols, as d. For each dry particle size and composition, the critical supersaturation (SS_{c}) is evaluated as the maximum of the equilibrium droplet growth (Köhler) curve described by Eq. 1. The droplet size where SS_{c} occurs is here referred to as the critical droplet diameter d_{c}, or the *point of activation*. When droplets have grown past their respective critical point to sizes $d > d_{\mathrm{c}}$, they are described as *activated* cloud droplets. At earlier points $d \leq d_{\mathrm{c}}$ on the Köhler curves, droplets are considered to be in the process of *activating*.

The water activity (also called the Raoult term) describes the suppression of equilibrium water partial pressure over an aqueous solution by dissolved solutes, compared to the saturation vapor pressure of pure water, as

$$p_{\mathrm{w}} = a_{\mathrm{w}} p_{\mathrm{w}}^{0} = \gamma_{\mathrm{w}} x_{\mathrm{w}} p_{\mathrm{w}}^{0}\,. \tag{2}$$

Here, x_{w} is the water (mole or mass) fraction in solution and γ_{w} is the corresponding (mole or mass fraction based) activity coefficient of water. The exponential (or Kelvin) term describes the enhancement of vapor pressure over the convex side of a curved droplet surface, compared to a planar surface of the same liquid, and depends explicitly on the droplet surface tension. Both water activity and Kelvin term are functions of droplet composition, determining x_{w} and thus $\gamma_{\mathrm{w}} = \gamma_{\mathrm{w}}(x_{\mathrm{w}})$ and a_{w}, as well as any concentration dependent change in droplet solution surface tension from the pure water value, $\Delta\sigma = \sigma_{\mathrm{w}} - \sigma$.

The total (T) amount of solute in the growing droplets remains constant and is determined from the dry particle compositions in terms of relative mass fractions $W_{\mathrm{p,s}}$ of each solute s, where $\sum_{s} W_{\mathrm{p,s}} = 1$. Assuming volume additivity in spherical particles, the total dry mass of each solute is then given from their bulk mass densities ρ_s as

$$m_s^T = W_{\mathrm{p},s}\frac{\pi}{6}D_\mathrm{p}^3\left(\sum_j \frac{W_{\mathrm{p},s}}{\rho_j}\right)^{-1}. \tag{3}$$

In our calculations, we have used $\rho_\mathrm{NaCl} = 2.165\,\mathrm{g\,cm^{-3}}$ and $\rho_\mathrm{NAFA} = 1.6\,\mathrm{g\,cm^{-3}}$. The NAFA density is not available in the literature and is therefore assumed to be similar to that of Suwannee River Fulvic Acid, another common reference humic substance (Dinar et al., 2006a). In principle, this quantity can readily be determined by simple weighing of a well-defined volume of the sample, but the resulting value is highly dependent on the packing of the sample material and we have therefore refrained from obtaining a more precise experimental estimate here. The droplet temperature is assumed to be $T = 303$ K, reflecting the range of effective temperatures from about $298-313$ K in the CCN counter between measurements at different supersaturations (T.B. Kristensen, personal communication). The sensitivity of calculations to the assumed value of ρ_NAFA and variations in experimental droplet temperature is discussed in the Supporting Information (SI).

At each droplet size, the total amount of water is calculated by assuming volume additivity also of water and dry particle components within the droplet phase, as

$$m_\mathrm{w}^T = \rho_\mathrm{w}\frac{\pi}{6}(d^3 - D_\mathrm{p}^3)\,. \tag{4}$$

The total droplet composition $\{x_i^T\} = \mathbf{x^T}$ is then given in terms of the mass fractions of each component i as

$$x_i^T = \frac{m_i^T}{\sum_j m_j^T} \tag{5}$$

2.1 Surfactant partitioning

When surface active material adsorbs at the droplet surface, it leads to a partitioning of the total mass of surface active solute m_sft^T between the surface (S) and bulk (B) phases of the solution droplet. This partitioning depletes the droplet bulk concentration, compared to the total concentration $x_\mathrm{sft}^B < x_\mathrm{sft}^T$ and changes the overall bulk composition, compared to the total composition of the droplet $\{x_i^B\} = \mathbf{x^B} \neq \mathbf{x^T}$. To calculate the resulting amount of solute in the droplet bulk (and surface), we use a partitioning model based on the Gibbs adsorption equation (Gibbs et al., 1928) in the form:

$$RT\sum_i \frac{m_i^T}{M_i}\frac{\partial \ln(a_i)}{\partial m_\mathrm{sft}^B} + A\frac{\partial \sigma}{\partial m_\mathrm{sft}^B} = 0\,, \tag{6}$$

where $A = \pi d^2$ is the droplet surface area, m_i^T and M_i are the total and molar mass of each droplet component i, a_i is the activity of each component in the droplet solution, and m_sft^B is the mass of partitioning (surface active) species in the droplet bulk. For chemically well-defined components, here water and NaCl, M_i are well-known quantities. For NAFA, we here assume an average molar mass of $\bar{M}_\mathrm{NAFA} = 4266\ \mathrm{g\,mol^{-1}}$ according to the estimate of Mäkelä and Manninen (2008). This corresponds to an assumption of the average mass of a partitioning unit. The sensitivity of calculations to variations by up to an order of magnitude in the assumed value of $\bar{M}_\mathrm{NAFA}$ is discussed in the SI. Activities for non-volatile solutes are very challenging to measure directly, but can in binary solutions be inferred from measurements of the solvent activity *via* the

Gibbs-Duhem equation. Since this is not possible for ternary and higher-order mixtures, a_{NAFA} and a_{NaCl} are approximated as the corresponding mass fraction concentrations. Previous estimates for ternary surfactant–NaCl aqueous mixtures showed that this assumption had only minor effects in Köhler calculations (Prisle et al., 2010). The composition-dependent droplet water activity a_w, which also enters directly into Eq.1, is evaluated from an experimentally-based parameterization as described in Section 2.2.

The bulk/surface partitioning equilibrium is solved iteratively from Eq. 6 at each droplet size d and total composition $\mathbf{x^T}$, constrained by mass conservation for all droplet components, $m_i^T = m_i^B + m_i^S$, and by choosing the position of the Gibbs surface to yield the droplet bulk-phase volume equal to the total droplet volume, $V = \pi d^3/6$ (Prisle et al., 2010).

2.2 Ternary parametrizations

Iterations of critical supersaturations from Eq.1 require continuous functions for concentration-dependent variations in surface tension and water activity of the growing droplets. Here, both σ and a_{w} are described as functions of droplet bulk composition $\mathbf{x^B}$, which is the basis for using the Gibbs adsorption equation in the form given in Eq. 6. At equilibrium, the surface and bulk compositions of a given surface active substance are related via the concentration gradient resulting from its surface activity and mass conservation within the solution, just as the the activities of water and all other components are the same in all phases of the solution. Although the surface tension of a solution may also be given in terms of the surface composition (Ruehl et al., 2016), a major advantage of using bulk-composition based relations for solution properties is that these can be readily obtained from measurements for macroscopic solutions, where the bulk-phase composition is directly constrained in terms of the total dissolved mass. The absolute surface composition is on the other hand not easily quantified by direct measurement.

The key to applying composition-dependent properties obtained for macroscopic systems to finite-sized droplets, is to correct the bulk (or surface) concentrations of droplet components using a partitioning model. When partitioning of surface active solute to the droplet surface is considered, the bulk concentration changes along the Köhler growth curve, due to both dilution as the droplet grows and changing bulk/surface partitioning, for example expressed in terms of the surface partitioning factor $m_{\mathrm{sft}}^S/m_{\mathrm{sft}}^B$, with changing ratio of the droplet surface area and bulk volume. For ternary water–NAFA–NaCl droplet compositions, the relative solute mass fractions in the droplet bulk phase

$$w_s = \frac{m_s^B}{\sum_j m_j^B}\,, \tag{7}$$

where m_s^B is the mass of solute s in the droplet bulk and $\sum_s w_s = 1$, of NAFA and NaCl therefore change in a continuous fashion from the corresponding dry particle composition ($W_{\mathrm{p},s}$), as a result of changing NAFA partitioning in the growing droplets. The effect of bulk/surface partitioning is to move the droplet bulk (and surface) solution mixing state in the 2-dimensional NAFA–NaCl concentration domain, compared to the total droplet mixing state, or a macroscopic solution with the same composition. As a consequence, continuous parametrizations with respect to independent variations in all component concentrations are needed to evaluate droplet properties over the full range of mixing states realized during droplet growth and activation.

Parametrizations of both σ and a_w were obtained by fitting continuous functions of NAFA and NaCl aqueous concentrations to the experimental surface tensions and water activities reported by Kristensen et al. (2014) and Lin et al. (2020) for macroscopic solutions of same solute compositions as the original dry particles, using the least squares method. By using mass-based concentrations, which are readily available from experimental parameters, a quantitative description is obtained for all solution components, including the chemically unresolved NAFA.

2.2.1 Surface tension σ

NAFA–NaCl aqueous surface tensions (in $\mathrm{mN\ m^{-1}}$) were fitted with the Szyszkowski equation in the form (Meissner and Michaels, 1949):

$$\sigma = \sigma_\mathrm{w} - q_\mathrm{st1} \ln\left(1 + \frac{C_\mathrm{NAFA}}{q_\mathrm{st2}}\right), \tag{8}$$

where $\sigma_\mathrm{w} = 93.6635 + 0.009133\ T - 0.000275\ T^2$ (Dillmann and Meier, 1991; Vanhanen et al., 2008) is the temperature-dependent surface tension of pure water (in $\mathrm{mN\ m^{-1}}$) and C_NAFA is the mass concentration of NAFA (in $\mathrm{g\ L^{-1}}$). Dependency of σ on NaCl concentration enters through the fitting parameters q_st1 and q_st2, which are both functions of the relative NAFA–NaCl mass fraction in solution.

Kristensen et al. (2014) and Lin et al. (2020) report that measured aqueous NAFA surface tension decreases with time after formation of the sample surface. This is likely due to both dynamic effects of surface adsorption and structural rearrangements in the surface phase, as well as potentially to continually increased concentrations of the pendant drop samples from evaporation of water over the course of measurements. Fitting parameters for the surface tension parametrization (Eq. 8) used in the present calculations were obtained from measurement data corresponding to times $t = 600$ s after generation of the pendant drops. Following considerations of Prisle et al. (2008), the ratio of these measurement times to those of the cloud droplet activation measurements is here estimated to be roughly of the same order of magnitude as the diameter ratio of the droplets involved in the two types of measurement ($\sim 10^2$). With this simple argument, any potential dynamic effects of surfactant solute diffusing to the droplet surface, leading to incomplete (non-equilibrium) NAFA partitioning, are assumed to be at least comparable between the surface tension parametrizations and the droplet activation measurements, if present at all. Using a comprehensive set of time-evolving surface tension measurements for aqueous NAFA–NaCl mixtures with a wide range of compositions, Lin et al. (2020) presented a detailed assessment of the effects of time-dependent surface adsorption in Köhler calcuations. At the selected time lapse of $t = 600$ s, measurement data were available from Kristensen et al. (2014) and Lin et al. (2020) for the widest range of solutions, and generally the steepest and the majority of the total surface tension decrease with respect to measurment time had occurred at this point.

The surface tension fitting parameters q_st1 (in $\mathrm{mN\ m^{-1}}$) and q_st2 (in $\mathrm{L\ g^{-1}}$) for times $t = 600$ s are given as

$$q_\mathrm{st1} = 10.46 - 4.810\ w_\mathrm{NAFA} \tag{9}$$

and

$$q_\mathrm{st2} = 0.5947 - 0.3278\ w_\mathrm{NAFA}, \tag{10}$$

where w_{NAFA} is the (dimensionless) mass fraction of NAFA solute relative to NaCl in the solution bulk phase given in Eq. 7. Fits were made with the constraints that $q_{\mathrm{st1}} \geq 0$ and $q_{\mathrm{st2}} > 0$ for all $w_{\mathrm{NAFA}} \in 0-1$.

We also made ternary fits to the surface tension data using the Szyszkowski-type equation given by Prisle et al. (2010), which contains an additional term explicitly including the positive aqueous surface tension gradient with respect to NaCl concentration, as well as having both fitting parameters depend quadratically, instead of linearly, on w_{NAFA}. The more elaborate equations did not significantly improve the fit to data, while introducing several additional fitting parameters to the model. In our calculations, we therefore used the simpler Eq. 8 with implicit NaCl dependency and linear variation of the fit parameters with w_{NAFA}.

2.2.2 Water activity a_w

Osmolality-derived water activities were fitted as functions of NaCl and NAFA mass concentrations (C_{NaCl} and C_{NAFA}, both in g L^{-1}) in the form:

$$a_{\mathrm{w}} = 1 + q_{\mathrm{a1}} C_{\mathrm{NaCl}} + q_{\mathrm{a2}} C_{\mathrm{NAFA}}\,, \tag{11}$$

with fitting parameters $q_{\mathrm{a1}} = -5.68 \cdot 10^{-4}$ L g^{-1} and $q_{\mathrm{a2}} = -2.68 \cdot 10^{-5}$ L g^{-1}. Several other, more complex functions were tested as well, but the simple linear relations gave the most reasonable fits to the data over the measured composition ranges. Water actvities derived from osmometry in principle include all non-ideal solution effects, in particular concentration-dependent NAFA dissociation and effects of any non-ideal interactions among the resulting solute entities. Still, the linear relationship on mass concentrations of solute with unknown molar content may not be thermodynamically consistent over the full range of water–NAFA–NaCl mixing states. Indeed, for the limiting case of binary solutions, Eq. 11 does fail to comply with the Gibbs-Duhem relation in the limit of pure NAFA ($m_{\mathrm{w}} = m_{\mathrm{NaCl}} = 0$). This state is, however, never realized in our calculations, where droplet growth is initiated at a finite growth factor and tends toward infinite dilution. Zamora and Jacobson (2013) derived water activities from measured hygroscopic growth factors for NAFA–NaCl mixtures and also found near-linear relationships between water activity and total solute (molal) concentration.

2.3 Surfactant representations

For each dry particle composition and size, cloud droplet activation is calculated by considering the influence of NAFA surface activity according to five different representations (summarized in Table 1):

- **(P)** The full partitioning model decribed in Section 2.1: For each droplet size, the NAFA bulk/surface partitioning equilibrium is solved iteratively from Eq. 6 to determine the droplet bulk phase composition $\{x_i^B\} = \mathbf{x^B}$, from which droplet surface tension and water activity are evaluated according to concentration-dependent ternary parametrizations, $\sigma = \sigma(\mathbf{x^B})$ and $a_{\mathrm{w}} = a_{\mathrm{w}}(\mathbf{x^B})$, according to Eqs. 8 and 11. By using measurement-based parametrizations which rely only on *mass* concentrations and mass mixing ratios of organic and inorganic components, a quantitative description is obtained with respect to all droplet components, including the chemically unresolved NAFA. This comprehensive thermodynamic formulation serves as a benchmark for the evaluation of effects of NAFA surface activity in cloud droplet activation, as well as for the performance of the other representations applied.

- **(S)** The simple partitioning model of Prisle et al. (2011): All surfactant solute is assumed to be completely partitioned to the droplet surface, such that $m^B_{\mathrm{sft}} = 0$ for all droplet sizes and compositions, and the surface active particle components do not affect either water activity or surface tension at the point of activation. This representation is a simple empirical model based on the predictions of the thermodynamically consistent partitioning model of Prisle et al. (2010) for droplets comprising simple, strong, molecular surfactants (such as SDS) at the critical point of activation. Because the surface active components do not contribute to the composition-dependent droplet properties and the partitioning equilibrium does not need iteration, this representation is computationally simple and immediately applicable to chemically unresolved complex surface active mixtures. When all surfactant mass is depleted from the bulk, concentration-dependent droplet water activity is evaluated from the binary aqueous NaCl parametrization given by (Prisle, 2006) based on data from Low (1969):

$$a_{\mathrm{w}} = 1 - 0.031715 b_{\mathrm{NaCl}} + 0.0012582 b^2_{\mathrm{NaCl}} - 0.000022921 b^3_{\mathrm{NaCl}}. \quad (12)$$

  Here, b_{NaCl} is the molal concentration of NaCl, which is readily determined from the mass concentration *via* the well-known molar mass of NaCl. Droplet surface tension is constant $\sigma = \sigma_{\mathrm{w}}$.

- **(I)** Insoluble surfactant model: Similar to (S), all surfactant solute is assumed to be completely partitioned to the droplet surface ($m^B_{\mathrm{sft}} = 0$), but the surface tension is reduced by a constant amount to either $\sigma = 0.95\sigma_{\mathrm{w}}$ or $0.80\sigma_{\mathrm{w}}$ throughout droplet growth. This corresponds to a simplified representation of an insoluble surfactant, where the surface active component does not dissolve into the bulk solution, but forms a phase-separated layer on the surface which reduces solution surface tension according to the surface coverage (Ruehl et al., 2016). Due to the lack of quantitative surface-composition based surface tension relations for chemically unresolved NAFA, the surface tension reduction is here represented with a constant value.

- **(B)** Bulk solution model: The droplet is assumed to have the same properties as a macroscopic (bulk) solution with corresponding total composition. The surface partitioning factor is assumed to be negligible, such that the droplet bulk phase composition is determined directly from the total composition without iteration ($\mathbf{x^B} = \mathbf{x^T}$). Droplet surface tension and water activity are evaluated according to the same concentration-dependent mass-based ternary parametrizations given in Eqs. 8 and 11 as for **(P)**. However, the bulk compositions at each droplet size will generally differ between the two representations.

- **(K)** Basic Köhler model: Effects of surface activity are disregarded altogether. As for **(B)**, the droplet bulk phase composition is equal to the total droplet composition, without correction for surface partitioning ($\mathbf{x^B} = \mathbf{x^T}$). The surface tension is assumed to be constant for all droplet sizes and compositions and equal to that of pure water ($\sigma = \sigma_{\mathrm{w}}$). Droplet water activity is evaluated according to the concentration-dependent mass-based ternary parametrization in Eq. 11, using the total droplet composition $a_{\mathrm{w}} = a_{\mathrm{w}}(\mathbf{x^T})$.

Table 1. Properties included in the different representations of NAFA surface activity used in Köhler calculations.

model	partitioning	$\sigma = \sigma_\mathrm{w}(\mathbf{x^B})$	$a_\mathrm{w} = a_\mathrm{w}(\mathbf{x^B})$
(P) full partitioning	Eq. 6	Eq. 8	Eq. 11
(S) simple partitioning	$m^B_\mathrm{NAFA} = 0$	σ_w	Eq. 12
(I) insoluble surfactant	$m^B_\mathrm{NAFA} = 0$	$0.80\sigma_\mathrm{w}, 0.95\sigma_\mathrm{w}$	Eq. 12
(B) bulk solution	no, $\mathbf{x^B} = \mathbf{x^T}$	Eq. 8	Eq. 11
(K) basic Köhler	no, $\mathbf{x^B} = \mathbf{x^T}$	σ_w	Eq. 11

Representations (P), (S), and (I) include considerations of the impact of surface adsorption on bulk/surface partitioning, whereas (B) and (K) are both bulk solution representations. Surface tension is reduced in (P) and (B) according to composition dependent relations, and by a constant value in (I). As the surface active component is completely partitioned to the surface in (S) and (I), only NaCl impacts water activity in these representations, whereas ternary water activity relations are used in (P), (B), and (K).

Strictly, only representation (P) requires the use of fully continuous ternary parametrizations, since only in these calculations does the relative NAFA–NaCl solute mixing ratio change from that of the dry particles as the droplets grow ($w_i \neq W_{\mathrm{p},i}$). In representations (S) and (I), the relative bulk phase mixing state of NAFA and NaCl changes discontinuously at the onset of droplet growth, from the nominal dry particle value to $\{w_\mathrm{NAFA} = 0, w_\mathrm{NaCl} = 1\}$ in droplets where NAFA is completely partitioned to the surface. When representations (B) and (K) are used, the relative mixing ratio of NAFA and NaCl solutes remains equal to the nominal value of the dry particles and does not change with concentration of the growing droplets ($w_i = W_{\mathrm{p},i}$). The individual binary parametrizations (1-dimensional composition space) given for each nominal NAFA–NaCl solute mixing ratio by Kristensen et al. (2014) could therefore in principle be employed in these cases. For consistency, the ternary parametrizations given in Eqs. 8 and 11 are here used in all calculations, at essentially no additional computational cost. This allows us to compare features of the different surfactant representations, in terms of predicted droplet properties for continuous variation in dry particle compositions.

3 Results and discussion

In the following, we present results of modeled CCN activity and droplet properties during growth and at the critical point of activation for mixed NAFA–NaCl particles, using the different representations of NAFA surface active properties in aqueous solution droplets. By analyzing and comparing the results of each representation, various effects of NAFA surface activity on predicted CCN activity are assessed. Model sensitivity to selected input parameters, including assumed NAFA mass density and average molar mass, droplet temperature, choice of surface tension equation, and the effect of potential sample impurity in the droplet activation measurements of Kristensen et al. (2014) is presented in the SI.

3.1 CCN activity

Modeled critical supersaturations (SS_c) as functions of dry particle diameter (D_p) are presented in Figure 1 for particles with dry NAFA mass fractions ($W_\mathrm{p,NAFA}$) of 0% (blue), 20%, (green), 50% (red), 80% (purple), and 100% (black), relative to NaCl. Results of Köhler calculations with each of the four representations of surfactant effects (P), (S), (B), and (K) are shown in panels a), b), c), and d), respectively, together with the experimental values for particles with equivalent dry compositions reported by Kristensen et al. (2014) for comparison. Error bars on the experimental data are estimated as ± 1 standard deviations on measured SS_c, as reported by Kristensen et al. (2014). Model results for representation (I) are shown in the SI.

All representations of NAFA surface activity give similar results in the limit of pure NaCl particles, as expected. For each representation, the modeled CCN activity decreases (SS_c increases) with increasing $W_\mathrm{p,NAFA}$ for a given particle size, in agreement with the experimental trend. This shows that upon varying the dry particle composition from pure NaCl to pure NAFA, any effect of decreased droplet surface tension at the point of activation, from the presence of surface active NAFA in the droplet phase, cannot overcome the simultaneous increase in water activity (Eq. 2), arising from a potential combination of *i*) increasing droplet non-ideality (specifically leading to increased $\gamma_\mathrm{w} > 1$), *ii*) depletion of solute from the droplet bulk phase due to NAFA surface partitioning, and *iii*) the much higher average molar mass of NAFA, compared to pure NaCl (both leading to increased x_w^B). Several studies have previously observed the same trend, experimentally or in model calculations, for aerosol systems comprising both simple strongly surface active molecules, such as SDS and fatty acid sodium salts, as well as complex macromolecules and surface active mixtures, in various mixing ratios with NaCl (Li et al., 1998; Prisle et al., 2008, 2010; Hansen et al., 2015; Petters and Petters, 2016; Dawson et al., 2016; Forestieri et al., 2018; Prisle et al., 2019).

The overall good performance of calculations using (P) are reassuring in terms of our ability to capture relevant properties of the activating droplets within the comprehensive thermodynamic description. Each of the representations (P), (S), and (K) describe the experimental data fairly well, except in the case of pure NAFA particles, where (P) and (S) underestimate CCN activity well outside the reported experimental uncertainty. In the absence of hygroscopic NaCl, predictions with model (S) correspond to condensation of water into a pure aqueous droplet phase in the presence of insoluble material, which is adsorbed at the droplet surface without attaining full coverage. Similarly for the insoluble surfactant model (I), shown in Fig. S3 in the SI, but here the reduced surface tension brings predictions somewhat closer to experimental values for pure NAFA particles, compared to (S). To reconcile predictions of model (I) with measured SS_c for pure NAFA particles would however require much stronger surface tension reductions than the 5–20% included in the present calculations, at the expense of increasingly poor agreement with experimental values for all other particle compositions. In general, it is clear that model (I) does not represent experimental CCN data well across the full range of NAFA–NaCl particle sizes and compositions investigated. This suggests that discrepancies observed for the other partitioning models (P) and (S) with respect to pure NAFA particles cannot be attributed to surface tension effects alone. It is possible that relatively small amounts of hygroscopic impurities could be present in the organic aerosol mass and thus enhancing experimental CCN activity, as described by Bilde and Svenningsson (2004). The model sensitivity analysis presented in the SI shows that even 3% by mass of impurities in the NAFA mixture with hygroscopic properties corresponding to those of NaCl would be sufficient to reconcile the calculations of model (P) with

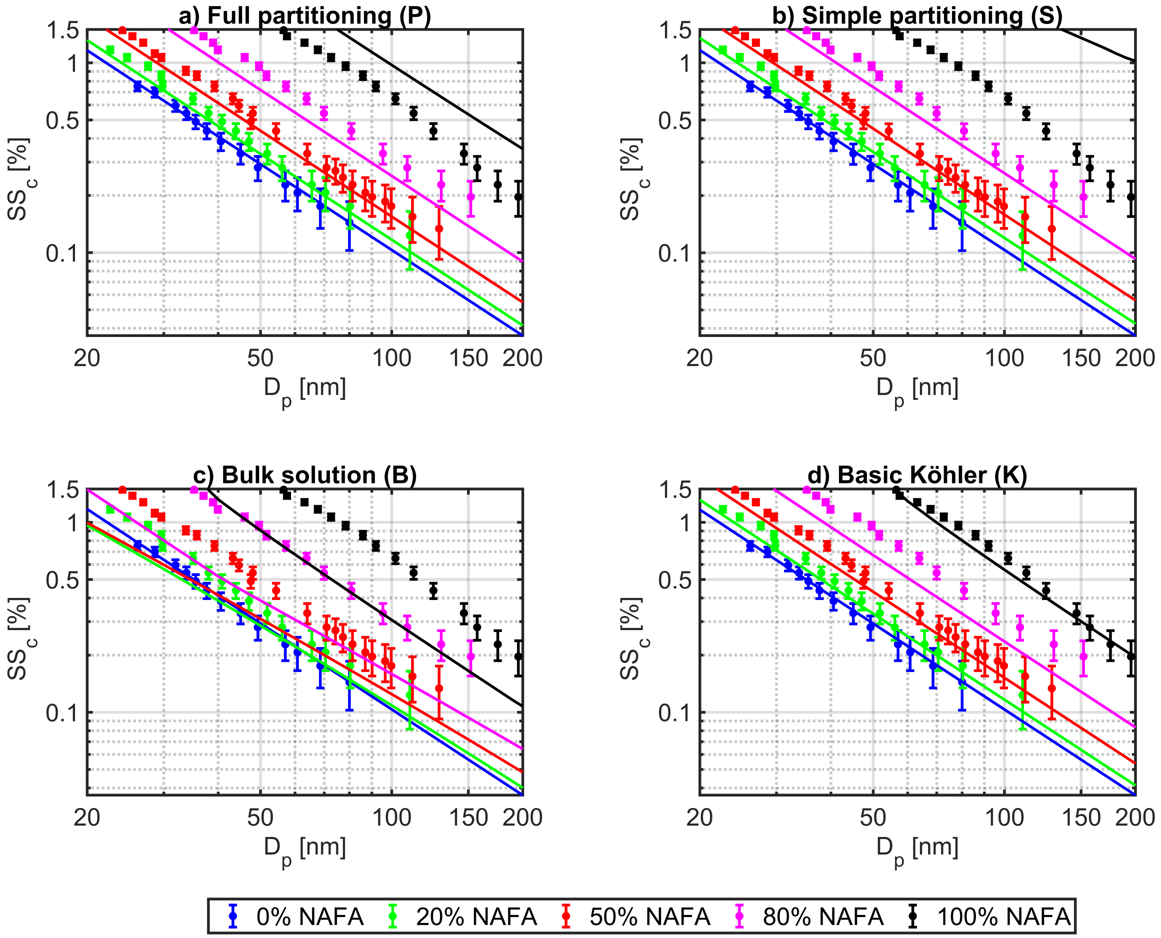

Figure 1. Critical supersaturations (SS_c) for mixed NAFA–NaCl particles, calculated (curves) using the different representations of NAFA surface activity described in Section 2.3: (a) full partitioning model (P), (b) simple partitioning model (S), (c) bulk solution model (B), and (d) basic Köhler model (K), in each case compared to experimental values (dots) measured by Kristensen et al. (2014). Colors indicate original dry particle fraction of NAFA ($W_\mathrm{p,NAFA}$) relative to NaCl. Calculations are made using a NAFA mass density of $\rho_\mathrm{NAFA} = 1.6\ \mathrm{g\ cm^{-3}}$. Error bars on experimental data represent ±1 standard deviations on SS_c as reported by Kristensen et al. (2014).

experimental data for pure NAFA particles. Model (K) tends to overestimate mixed NAFA–NaCl CCN activity slightly more than (P) and (S), hinting that NAFA bulk depletion from surface partitioning may indeed have a more significant impact on decreasing CCN activity than surface tension reduction has on increasing it.

The most prominent feature of Fig. 1 is how Köhler calculations using the bulk solution representation (B) clearly and consistently underestimate experimental critical supersaturations for all particle sizes and compositions. Similar observations 5 have been made in several previous studies at sub- and supersaturated conditions of particles comprising both chemically simple and complex surfactants and for both pure surfactant particles and in various mixtures with inorganic salts (Li et al., 1998; Rood and Williams, 2001; Sorjamaa et al., 2004; Prisle et al., 2008, 2010; Harmon et al., 2010; Ruehl et al., 2010; Zamora and Jacobson, 2013; Kristensen et al., 2014; Hansen et al., 2015; Petters and Petters, 2016; Forestieri et al., 2018; Prisle et al., 2019). Thus, the dramatic increase in CCN activity initially anticipated from the results of Facchini et al. (1999), by including aerosol surface activity equivalent to macroscopic solutions in the Köhler framework, was found also for these particles comprising a more complex atmospherically relevant surface active mixture to not reproduce experimental CCN observations.

Kristensen et al. (2014) compared their measured CCN activities to two simple Köhler models based on similar assumptions as representations (B) – macroscopic solution, concentration-dependent surface tension and water activity – and (K) – macroscopic solution, constant surface tension equal to that of pure water and concentration-dependent water activity – of the present work, with some differences in the actual model implementation. In this work, models (B) and (K) are used for reference to predictions with the full partitioning model (P) and therefore for consistency run with the continuous ternary surface tension and water activity parametrizations presented in Eqs. 8 and 11, even if these are not needed in absence of bulk/surface partitioning calculations. Kristensen et al. (2014) used simpler parametrizations with a 1-dimensional composition domain, which are not continuous with respect to variations in the relative NAFA–NaCl mass fractions w_{NAFA} and w_{NaCl} and have slightly different forms than the full ternary functions used here, even at the lines of intersection. Furthermore, the surface tension parametrizations used by Kristensen et al. (2014) are made for data points corresponding to measurement times t= 0 s after the formation of the surface and therefore based on higher surface tension values for a given solution composition, compared to the data from measurement times t= 600 s used in this work. As higher macroscopic surface tensions correspond to lower surface activity of NAFA, predictions of SS_{c} will similarly be biased higher, in the absence of partitioning considerations. Our calculations with model (B) would therefore also be closer to the experimental values of Kristensen et al. (2014) if we had used their surface tension parametrizations, but as clearly seen from Fig. 7 in Kristensen et al. (2014), this would still not bring model predictions even close to agreement with experiments.

Similar to the present model (K), Kristensen et al. (2014) also find that a basic Köhler model, where NAFA surface activity is completely ignored, gives good agreement with measured CCN activity for NAFA–NaCl particles with up to 50% NAFA, as well as for pure NAFA, but not for particle mixtures with 80% NAFA. This seemingly counter-intuitive result for particle mixtures comprising strongly surface active material with significant ability to lower surface tension in macroscopic solutions has previously been seen also for simple, strong surfactants, such as SDS and C8-C12 fatty acid salts (Sorjamaa et al., 2004; Prisle et al., 2008, 2010, 2011). On the other hand, several recent studies have shown properties for both simple and complex atmospheric aerosol, e.g. secondary organic aerosol (Ruehl et al., 2016), marine primary organics (Ovadnevaite et al., 2017), limonene-derived organosulfate products (Hansen et al., 2015), and water-soluble pollen extracts (Prisle et al., 2019) which are consistent with an enhancement of aerosol hygroscopicity by surfactants, at least partly due to reduced surface tension. This suggests that model (K) is likely too simple to fully capture CCN activity of different types of surface active material across all atmospherically relevant particle compositions and conditions and that, generally, a full partitioning model is needed for robust predictions. In cases where the basic Köhler model (K) gives good agreement with experimental CCN activity, it also closely traces predictions with the comprehensive partitioning model (P).

3.2 Droplet properties at activation

Figure 2a presents critical supersaturations for 50 nm dry particles calculated with each model representation as a function of NAFA mass fraction $W_{\mathrm{p,NAFA}}$ in the dry particles. Experimental values from Kristensen et al. (2014) for particles with similar dry sizes are shown for reference. Immediate comparison with experimental values is not always possible along the particle composition dimension, as Kristensen et al. (2014) did not measure the exact same particle sizes for each dry particle composition. This is because they used an experimental setup scanning a set of pre-selected supersaturations, rather than particle sizes. Corresponding to each value of SS_{c} shown in panel (a), other panels in Fig. 2 show for the same 50 nm particles: (b) the individual Kelvin and Raoult terms, (c) droplet diameter growth factor $GF_{\mathrm{c}} = d_{\mathrm{c}}/D_{\mathrm{p}}$, and (d) droplet surface tension σ_{c}, also calculated at the critical point d_{c} of the Köhler curve. Qualitatively similar results were obtained for other dry particle sizes, but model differences are more pronounced for smaller particles, which generally activate for smaller critical sizes, corresponding to smaller critical growth factors, with more concentrated droplet compositions and larger surface area-to-bulk volume ratios, introducing more pronounced surface partitioning for a given total composition.

Results in Fig. 2 illustrate how the simple representations (S) and (I), as well as the basic Köhler model (K) all predict very similar properties of activating droplets to those of the comprehensive partitioning model (P) for essentially the entire range of NAFA mass fractions in the particles. Not only critical supersaturations, but also the individual Kelvin and Raoult terms at the point of droplet activation, are fairly similar and predicted droplet sizes at activation (as represented by the droplet growth factors) also agree well. This was not immediately expected, since model (S) was proposed to emulate specifically SS_{c}, not necessarily other droplet properties at the critical point (Prisle et al., 2011), and since NAFA is seen from experimental data to give significant surface tension reductions in macroscopic solutions (Kristensen et al., 2014), contrary to the assumptions of both (S) and (K). The similarity of all activation parameters indicates that the underlying assumptions of both the simple representations and the basic Köhler model are reasonably representative for the NAFA particle systems in question, as predicted by the comprehensive model (P). This close agreement between basic Köhler predictions and comprehensive partitioning thermodynamics was also observed in previous studies for mixed surfactant–NaCl particles with SDS and fatty acid salts (Prisle et al., 2010, 2008). For NAFA particles, the agreement extends to even larger surfactant fractions (up to about 80% by mass of NAFA) than seen in these earlier studies, where models agreed for dry particle surfactant mass fractions up to about 50%.

It is important to note that properties in Fig. 2 correspond to critical droplets of different sizes d_{c}. Therefore, in addition to the overall variation in total solute composition given by $W_{\mathrm{p,NAFA}}$, also the droplet dilution state, as reflected in the varying activation growth factors GF_{c} (panel c), and the ensuing size-dependent bulk/surface partitioning of NAFA predicted with representation (P) vary between the droplets. Total composition, dilution, and partitioning each affect the droplet bulk solution composition, from which the droplet surface tension (panel d) and Kelvin and Raoult terms (panel b) are evaluated. Variations of critical droplet properties with $W_{\mathrm{p,NAFA}}$ therefore do not *a priori* reflect continuous variation in all underlying droplet properties, as they represent only the maxima of individual Köhler curves corresponding to each particle composition.

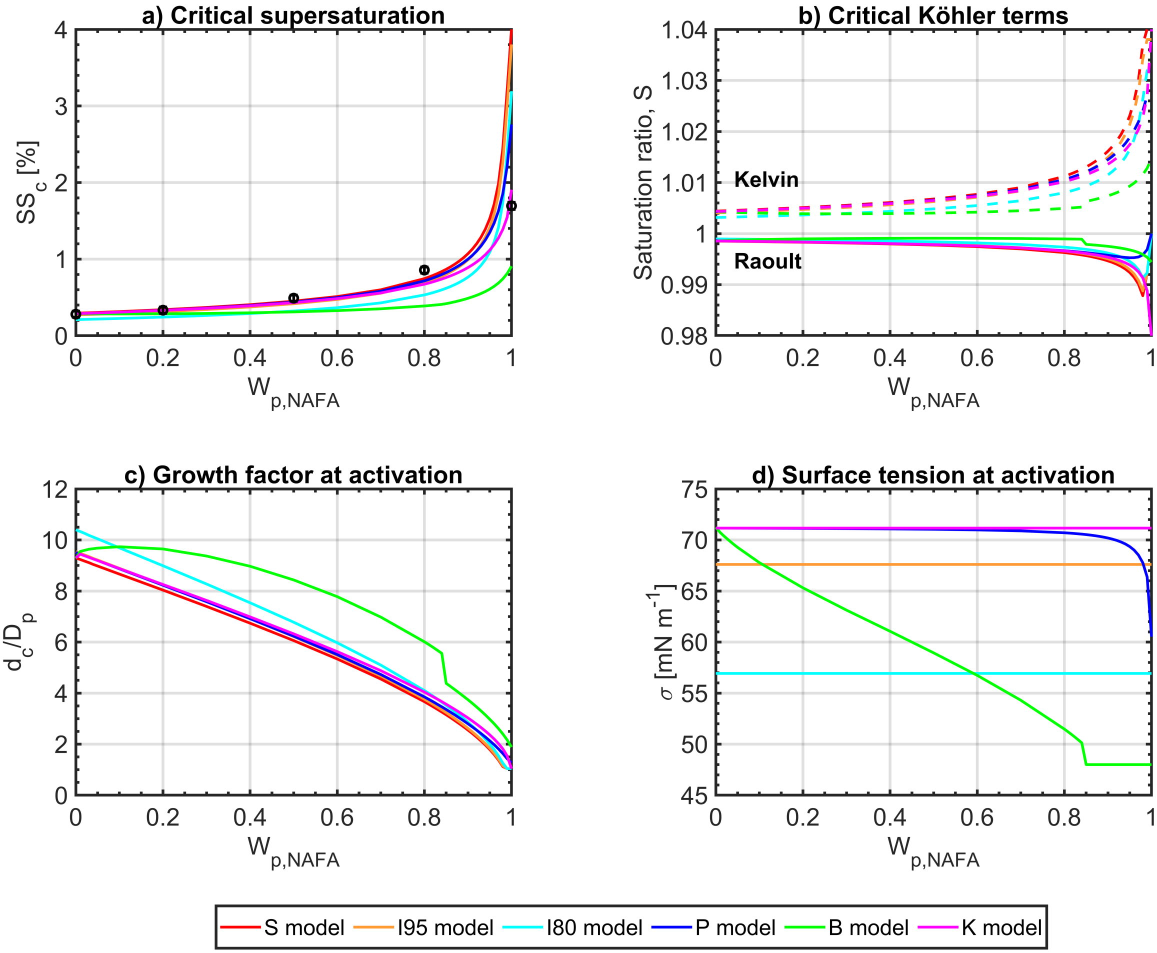

Figure 2. Properties of activating droplets calculated with representations (P), (S), (I), (B) and (K) at the critical point of droplet activation d_c for 50 nm dry particles as functions of dry particle NAFA mass fraction $W_\mathrm{p,NAFA}$: (a) critical supersaturations SS_c, (b) Kelvin and Raoult terms corresponding to each SS_c at the critical point of the Köhler curve, (c) droplet diameter growth factor, and (d) droplet surface tension. In panel (a), experimental values from Kristensen et al. (2014) for particles with similar dry sizes are shown for reference.

The Raoult terms shown in Fig. 2b each vary as functions of $W_\mathrm{p,NAFA}$, replacing hygroscopic NaCl with the significantly less hygroscopic component NAFA, as well as the critical droplet dilution state, both affecting the overall amount of water and solute in the droplets, and in the case of representations (P), (S), and (I) also the extent of NAFA bulk/surface partitioning. Each affect the composition of the droplet bulk phase, which govern a_w according to Eq. 2 in general and Eqs. 11 or 12 for the present calculations in particular. The calculated critical Raoult terms are seen to be *higher* for the bulk solution representation (B) than the other representations, despite that (P), (S) and (I) consider bulk depletion of NAFA, whereas (B), like (K), does not. This is due to the significantly higher dilution factor of activating droplets predicted by (B), as is seen from GF_c in Fig. 2c. For representations (P), (S) and (I), both Raoult terms and growth factors of activating droplets are very similar. For all representations, the predicted reduction of water activity at droplet activation is modest across the dry particle composition range.

For representations (P), (S), and (I), an infliction point is seen in the Raoult terms for very high $W_\mathrm{p,NAFA}$, whereas for (B) and (K), the Raoult terms decrease with increasing $W_\mathrm{p,NAFA}$ throughout the dry particle composition range. In the absence of bulk/surface partitioning, droplet concentrations continue to increase with decreasing dilution of the total solute mass, as seen from the growth factors GF_c Fig. 2c. When NAFA bulk/surface partitioning is considered, the effect of decreasing dilution is first strong enough to overcome the decrease in total amount of hygroscopic material with increasing $W_\mathrm{p,NAFA}$ and the depletion of NAFA from the droplet bulk, leading to decreasing Raoult terms, but eventually the balance reverses, as the total amount of NaCl becomes too small to compensate for the surface active component which is largely depleted from the bulk. With the full partitioning model, the Raoult term changes smoothly, whereas sharp infliction points are seen for the simple models (S) and (I), where partitioning occurs as a step function. Bulk compositions of activating droplets are discussed in more detail related to Fig. 3 below.

For representation (B), the Raoult term has a step change with respect to dry particle composition for $W_\mathrm{p,NAFA} = 0.85$. The increasing concentrations of both NAFA and NaCl are clearly seen in Figs. 3a and b below. This is caused by a step decrease in the critical droplet growth factors GF_c (Fig. 2c), leading a to a simultaneous step increase in the Kelvin term (Fig. 2b). As seen in Fig. 2a, the opposing changes in the Kelvin and Raoult terms caused by decreasing d_c cancel out, so that the resulting SS_c change smoothly with $W_\mathrm{p,NAFA}$. At the same dry particle composition, critical droplet surface tensions σ_c predicted with representation (B) reach a constant minimum value in Fig. 2d. This corresponds to droplets exceeding a critical micelle concentration-type transition for NAFA, which is estimated from the surface tension data of (Kristensen et al., 2014) to occur for various NAFA–NaCl mixtures at $\sigma = 48\ \mathrm{mN\ m^{-1}}$. Figures 4 and 5 (discussed in more detail below) show how the predicted critical point d_c shifts between two local maxima on the Köhler curve, from the larger to the smaller droplet size, corresponding to droplets with surface tensions above or at the minimum value, respectively. This causes the discontinuous shift in d_c and critical droplet properties seen for representation (B) in Figs. 2 and 3. A similar shift is not seen for calculations with representation (P), because droplet surface tension never reaches the minimum value $\sigma = 48\mathrm{mN\ m^{-1}}$ (Figs. 2d and 5).

The Kelvin term at droplet activation depends on the critical droplet size d_c, determining the curvature effect according to Eq. 1, together with the droplet surface tension as a function of droplet bulk composition, which in turn is governed by the droplet dilution state and size-dependent bulk/surface partitioning. The critical Kelvin terms for each NAFA representation in Fig. 2b generally follow the corresponding trends in d_c as given by GF_c (Fig. 2c). For representations (P), (S), and (I), GF_c values are mutually very similar across the entire dry particle composition range. Figure 2d shows how droplet surface tension at activation is reduced according to Eq. 8 in calculations with (P) and (B), or fixed to σ_w, $\sigma = 0.95\ \sigma_\mathrm{w} \approx 68\ \mathrm{mN\ m^{-1}}$, and $\sigma = 0.80\ \sigma_\mathrm{w} \approx 57\ \mathrm{mN\ m^{-1}}$ for models (K), (I95), and (I80), respectively. When the critical surface tension is significantly reduced in calculations with (B) and (I80), the corresponding Kelvin terms are somewhat lower than for (P), (S), and (I), where surface tension is only modestly reduced at activation, or not at all.

Predictions with representation (B) in Fig. 2d show that NAFA can significantly reduce surface tension of activating droplets when they are considered similar to macroscopic solutions, whereas for representation (P) the predicted surface tensions at droplet activation are overall only modestly reduced. For particles with less than 80% by mass of NAFA, the surface tensions in activating droplets are essentially the same as for pure water and only for the very highest mass fractions of NAFA ($W_{\mathrm{p,NAFA}} > 0.95$) is the surface tension reduced by more than 5% from the pure water value. This is one of the fundamental assumptions underlying calculations with both (S) and (K) – and the validity of this assumption as predicted with (P) for all but the largest dry particle NAFA fractions is one of the main reasons for the simultaneous close agreement between calculations using (S) and (K), and the comprehensive framework of (P). Furthermore, the effect of this modest surface tension reduction at the point of droplet activation must be more than counterbalanced by bulk depletion from NAFA surface partitioning, since the predicted SS_{c} are higher for (P) than for (K), but slightly higher in (S) than for (P), at the highest NAFA fractions. This is also reflected in the corresponding Raoult terms.

3.2.1 Bulk composition of activating droplets

Figure 3 presents mass concentrations of (a) NAFA and (b) NaCl in the droplet bulk, C_{NAFA} and C_{NaCl} (both in g L^{-1}) calculated at the critical point of activation d_{c} for the same particles with dry diameters of 50 nm and compositions $W_{\mathrm{p,NAFA}}$ as in Fig. 2. These are the solute concentrations governing the evaluated droplet surface tensions and water activities at activation. For the non-partitioning salt, C_{NaCl} is determined by the total amount of NaCl in the dry particle, given from $W_{\mathrm{p,NAFA}}$, and the droplet dilution state at activation, GF_{c} (Fig. 2c). For representations (P), (S) and (I), C_{NAFA} is in addition affected by bulk depletion from the size-dependent or step-wise bulk/surface partitioning. In calculations with (S) and (I), the bulk NAFA concentration is vanishing due to complete partitioning to the droplet surface, however, also for the comprehensive partitioning model (P) are NAFA bulk concentrations nearly vanishing at the point of activation across all dry particle compositions. As before, qualitatively similar results were obtained for other particle sizes. For larger particles, concentrations are even more dilute than those presented here for 50 nm particles.

In model (K), concentrations of *both* NAFA and NaCl in activating droplets increase with NAFA mass fraction in the dry particles, except for particles with the very largest dry NAFA fractions. This reflects how particles activate for still more concentrated droplet compositions, as seen in Fig. 2c. Across the all representations, evaluated C_{NaCl} at droplet activation for a given dry particle composition follow the trend in GF_{c}. In particular, for all representations except (B), activating droplets become more concentrated in the inorganic salt, even if $W_{\mathrm{p,NaCl}}$ decreases. For calculations with representation (B), C_{NAFA} increases with $W_{\mathrm{p,NAFA}}$ and decreasing GF_{c}, as expected. C_{NaCl} first decreases slightly, as the amount of NaCl in the particles decreases with increasing $W_{\mathrm{p,NAFA}}$, reflecting also a state of increasing, or relatively high, dilution, as activation occurs for large d_{c} when droplet surface tension is increasingly reduced (Fig. 2d). A discontinuous increase is seen with (B) for both C_{NAFA} and C_{NaCl} at $W_{\mathrm{p,NAFA}} = 0.85$, reflecting the sudden decrease in GF_{c} (Fig. 2c) as droplet activation shifts from the local maximum at larger, to that at smaller, d_{c} (Figs. 4 and 5). For all representations, C_{NaCl} show an infliction point for the largest $W_{\mathrm{p,NAFA}}$, where concentrations eventually fall, as decreasing dilution can no longer counter the decreasing total NaCl content in the droplets. This infliction point is visible in the Raoult terms of the partitioning representations (P), (S), and (I) seen in Fig. 2b, but not strong enough to translate into a similar infliction the Raoult terms of the bulk solution models (B) and (K).

The NAFA surface partitioning factor at droplet activation, in terms of the mass ratio of NAFA solute in the droplet surface and bulk, $m^S_{\mathrm{NAFA}}/m^B_{\mathrm{NAFA}}$, calculated with representation (P), is shown in Fig. 3c. In representations (S) and (I), this value is infinite at all droplet sizes, and in models (B) and (K), it is 0. Fig. 3d shows the resulting droplet bulk composition in terms of the mass fraction of solute comprised by NAFA, $w_{\mathrm{NAFA}} = m^B_{\mathrm{NAFA}}/(m^B_{\mathrm{NAFA}} + m^B_{\mathrm{NaCl}})$, at the point of droplet activation. For calculations with (B) and (K), this ratio is identical to the dry particle composition $W_{\mathrm{p,NAFA}}$, as it should in the absence of bulk depletion from surface partitioning of NAFA. With representations (S) and (I), the NAFA bulk solute fraction is vanishing, as $C_{\mathrm{NAFA}} = 0\ \mathrm{g\ L^{-1}}$ (Fig. 3a). Partitioning of NAFA profoundly changes the droplet bulk phase mixing state at the point of activation, compared to the relative NAFA–NaCl ratio in the original dry particles. For 50 nm particles in Fig. 3c, $m^S_{\mathrm{NAFA}}/m^B_{\mathrm{NAFA}}$ in activating droplets calculated from the comprehensive partitioning model (P) is larger than 500 for all particle compositions. For all dry particle sizes and NAFA mass fractions investigated (Fig. 1), calculated $m^S_{\mathrm{NAFA}}/m^B_{\mathrm{NAFA}}$ at the point of activation is greater than two orders of magnitude (not shown). As a result, except for the very largest dry particle NAFA fractions, the concentration of NAFA (Fig. 3a) and the relative amount of droplet solute comprised by NAFA (Fig. 3d) in activating droplets is all but vanishing.

These observations support the applicability of the underlying assumptions in the simple representation (S) for NAFA CCN activity, that the surfactant bulk concentration at droplet activation is effectively 0 and the overall impact of NAFA on particle hygroscopicity is vanishing.

3.3 Properties of growing droplets along Köhler curves

Figure 4 shows the Köhler curves for selected dry particle compositions $W_{\mathrm{p,NAFA}} =$ (a) 0.20, (b) 0.50, (c) 0.80, and (d) 0.95, calculated with each model representation for the 50 nm particles described in Figs. 2 and 3. The droplet surface tensions evaluated along the Köhler curves are shown in Fig. 5 and the corresponding NAFA surface partitioning factors $m^S_{\mathrm{NAFA}}/m^B_{\mathrm{NAFA}}$ and water activities of the growing droplets are presented in Figs. S4 and S5 of the SI. For all curves representing calculated properties of the growing droplets, the respective critical points of droplet activation (SS_{c}) presented in Figs. 1 and S3 are indicated with asterisks.

All representations used in calculations of CCN activity produce meaningful Köhler curves and other solution properties for the growing droplets. The close agreement between representations (P), (S), (I95) and (K) for calculated droplets properties at the point of activation d_{c} is seen in Fig. 4 along the full Köhler curves, expect for the highest NAFA fraction in the dry particles (panel d). For $W_{\mathrm{p,NAFA}} = 0.95$, clear differences in the shapes of the Köhler curves can be seen, as the differences between the NAFA representations become more prominent relative to the still smaller amount of hygroscopic NaCl in the droplets.

For both representations (I80) and (B), the predicted droplet surface tension is significantly reduced during droplet growth and well beyond the point of activation. At a given droplet size d, the equilibrium supersaturation SS is higher for representation (B) than for (I80) when the concentration-dependent droplet surface tension is higher in (B) than the fixed surface tension of $\sigma = 0.80\sigma_{\mathrm{w}}$ in (I80), and vice versa. When partitioning is included in the calculations with representations (P), (I95), and (S),

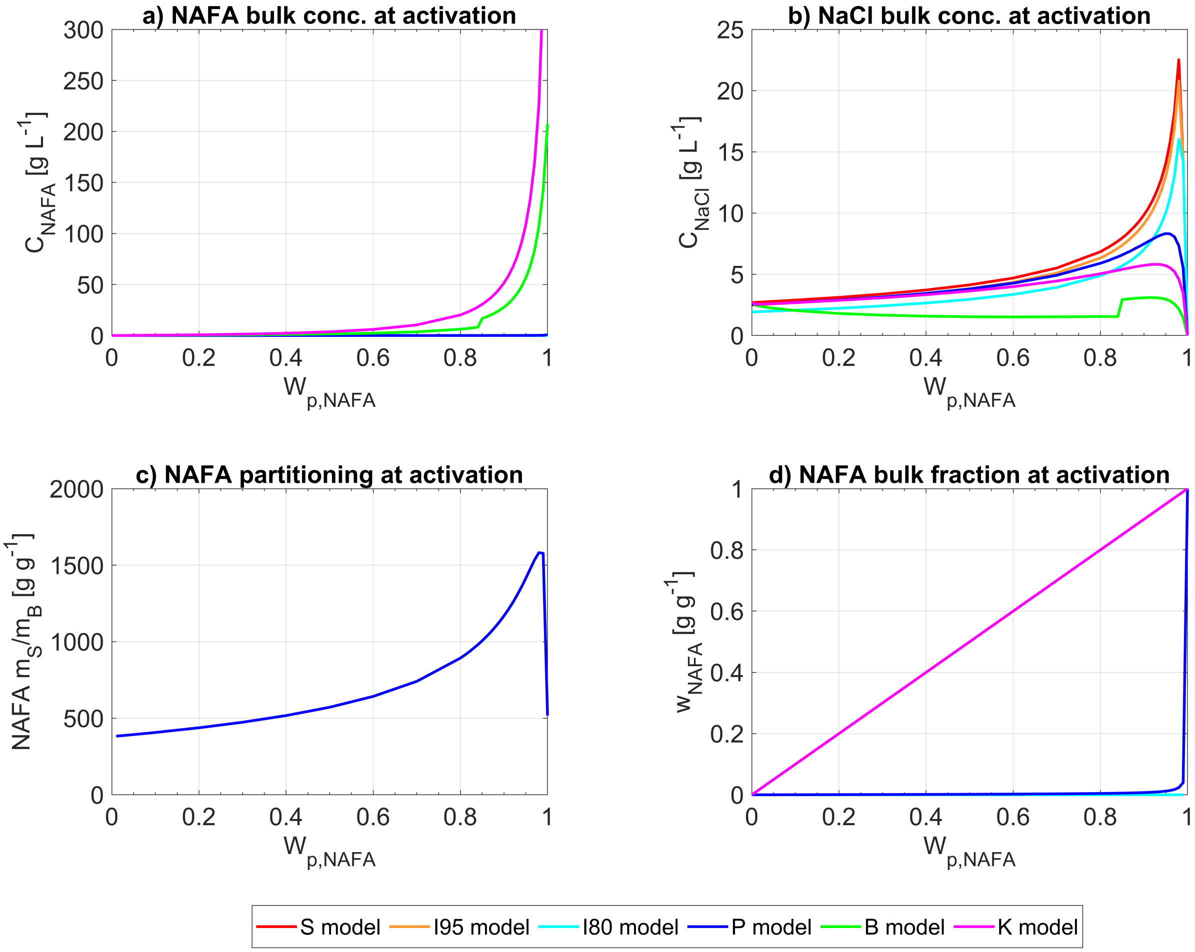

Figure 3. Mass concentrations C_i (in $\mathrm{g\,L^{-1}}$) of (a) NAFA and (b) NaCl in activating droplets calculated with the different representations (P), (S), (I), (B), and (K), for dry particles with diameters of 50 nm. For the same particles are also shown (c) NAFA surface partitioning factor $m^S_{\mathrm{NAFA}}/m^B_{\mathrm{NAFA}}$, and (d) mass fraction of bulk solute comprised by NAFA, $w_{\mathrm{NAFA}} = m^B_{\mathrm{NAFA}}/(m^B_{\mathrm{NAFA}} + m^B_{\mathrm{NaCl}})$, evaluated at the point of droplet activation.

the order of the Köhler curves at each d, as well as the values of SS_{c} at the critical points, do not simply follow the relative magnitudes of the droplet surface tensions. In calculations with representation (P), surface tension is reduced for the more concentrated droplets at the earlier stages of the Köhler growth curves, but only for the highest $W_{\mathrm{p,NAFA}}$ is the reduction maintained until the critical point. Even for droplets much smaller and more concentrated than at the point of activation ($d < d_{\mathrm{c}}$), surface tension is never reduced by more than about 10% from the pure water value. This reflects the very small amounts of NAFA solute remaining in the droplet bulk phase, when bulk/surface partitioning is taken into consideration.

The degree of partitioning to the surface is significant already at the much higher droplet concentrations at the early stages of the Köhler curves before activation and generally the amount of NAFA in the droplet surface is 2-3 orders of magnitude higher than the amount left in the bulk (Fig. S4). Typically, $m^S_{\mathrm{NAFA}}/m^B_{\mathrm{NAFA}}$ is even higher for droplet sizes $d < d_\mathrm{c}$ than at the critical point, illustrating that partitioning has even greater effect on droplet bulk concentration than smaller degrees of dilution in smaller droplets. As a consequence, even if NAFA is able to significantly reduce surface tension in macroscopic solutions, the same effect is not seen in microscopic activating droplets, even at similar total droplet concentrations. A comparison of surface tension variations predicted with Eq. 8 in macroscopic and microscopic droplet solutions due to changes in bulk composition from NAFA partitioning is discussed in more detail in the SI. Fig. S5 shows how droplet water activity increases as droplets grow and dilute along the Köhler curve. The water activity is significantly reduced early in droplet growth, but except for the largest $W_{\mathrm{p,NAFA}}$ is very close to 1 at d_c. Predicted droplet a_w only differ significantly between the different representations when NAFA fractions in the dry particles are very large. As NAFA is much less hygroscopic than NaCl, and the resulting reduction of water activity is even smaller for sub-micron droplets due to strong bulk/surface partitioning, a_w is governed by the hygroscopic salt and variations mainly reflect the varying droplet dilution state.

3.4 Consequences for Köhler modeling

The preceding discussion highlights how the comprehensive thermodynamic partitioning model (P) consistently during droplet growth and at the point of activation predicts the vast majority of NAFA in the droplet to be depleted from the bulk by partitioning to the surface. Except for particles with the very highest dry mass fractions, NAFA contributes next to none of the solute in the droplet bulk phase, which governs the equilibrium surface tension and water activity of the droplet. Even if NAFA effectively reduces surface tension in macroscopic solution, at droplet activation, the predicted surface tension is barely reduced at all for particles with less than 80% NAFA and for still higher NAFA fractions, the maximum surface tension reduction only amounts to around $10\ \mathrm{mN\ m^{-1}}$ from the pure water value across the investigated dry particle size range. For particles even smaller than those considered here, cloud droplet activation may occur for sufficiently small and therefore concentrated droplets that surface tension could be further reduced at d_c. However, extrapolating the experimental and modeling trends in Fig. 1, corresponding SS_c would be similarly higher (exceeding 1.5%) and likely represent supersaturation conditions which are rarely met in the atmosphere.

The basis for this seemingly counter-intuitive droplet state is the comparatively very large surface areas (A) relative to the finite volume (V) of the bulk for microscopic activating cloud droplets, compared to a macroscopic solution (Prisle et al., 2010; Bzdek et al., 2020). Even when essentially all the surface active material is adsorbed at the droplet surface, the finite-sized solution droplets do not comprise enough surface active solute altogether to generate sufficient surface concentrations to significantly reduce droplet surface tension. Predictions with the thermodynamic partitioning model show how adsorption to the large droplet surfaces depletes the bulk of surface active solute, leaving the resulting amount dissolved in the bulk phase at a given total concentration in the droplet essentially vanishing. The equilibrium bulk-to-surface concentration gradient governing the adsorption of a given surface active substance is therefore established for a droplet solution state of dilute concentrations in both bulk and surface phases. This leads to the strongly surface active component effectively behaving in small droplets as an

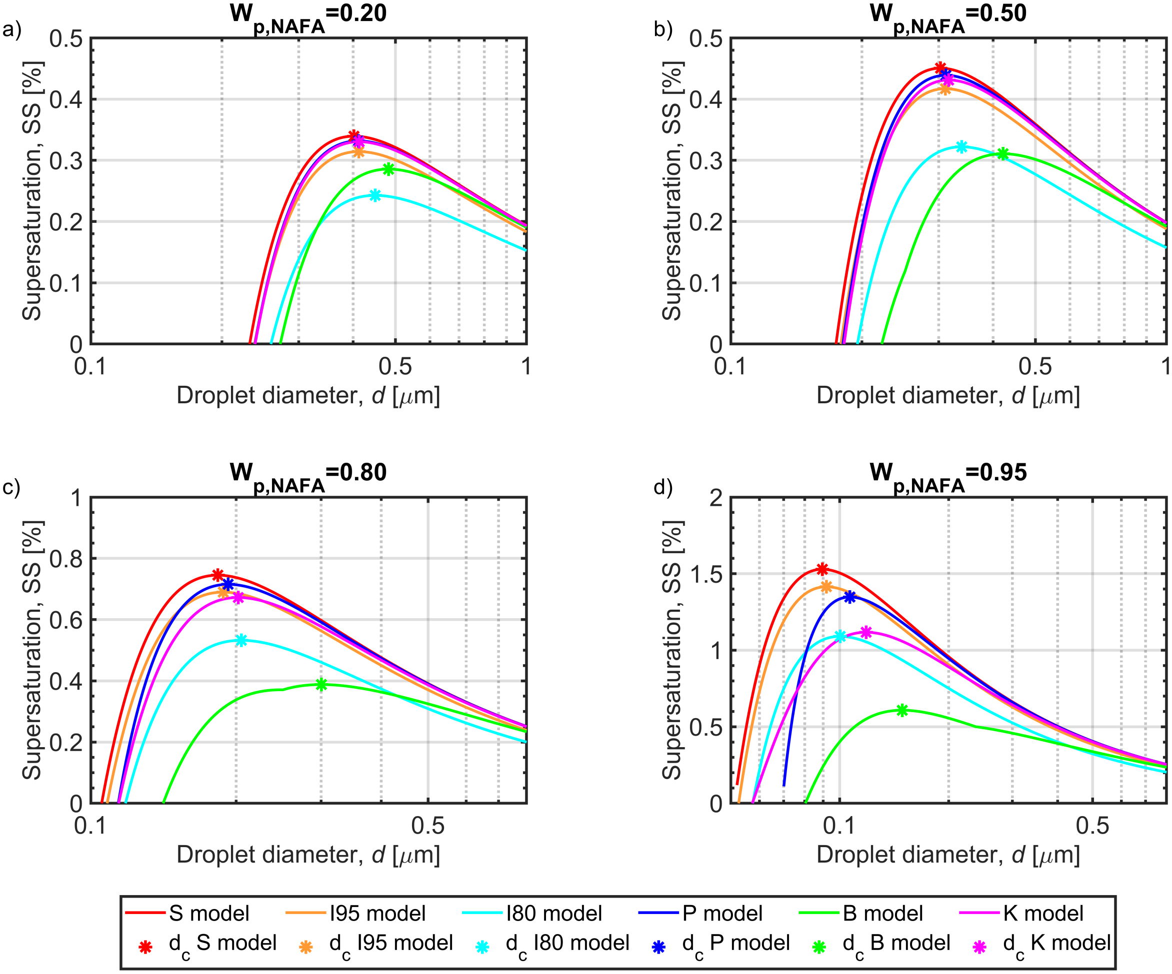

Figure 4. Köhler curves for growing aqueous NAFA–NaCl droplets formed from 50 nm dry particles with NAFA mass fractions of (a) 0.20, (b) 0.50, (c) 0.80, and (d) 0.95, calculated with the different models described in Section 2.3. The critical points of droplet activation (SS_c) presented in Figs. 1 and S3 are indicated with asterisks on each Köhler curve. Note that the supersaturation (SS) scale is different between the panels.

insoluble and slightly or even non-surface active substance. For NAFA in the present work, pronounced bulk phase depletion further diminishes the low intrinsic hygroscopicity, in terms of impact om bulk water activity, due to low aqueous solubility and large estimated average molar mass, to yield a nearly vanishing effective hygroscopicity in activating droplets.

These mechanisms explain the observed good performance of the simple partitioning model (S), where contributions from NAFA to both water activity and surface tension reduction are effectively set to zero, with respect to the comprehensive partitioning model (P). The simple model (S) is an empirical model developed to emulate the properties of strong surfactants

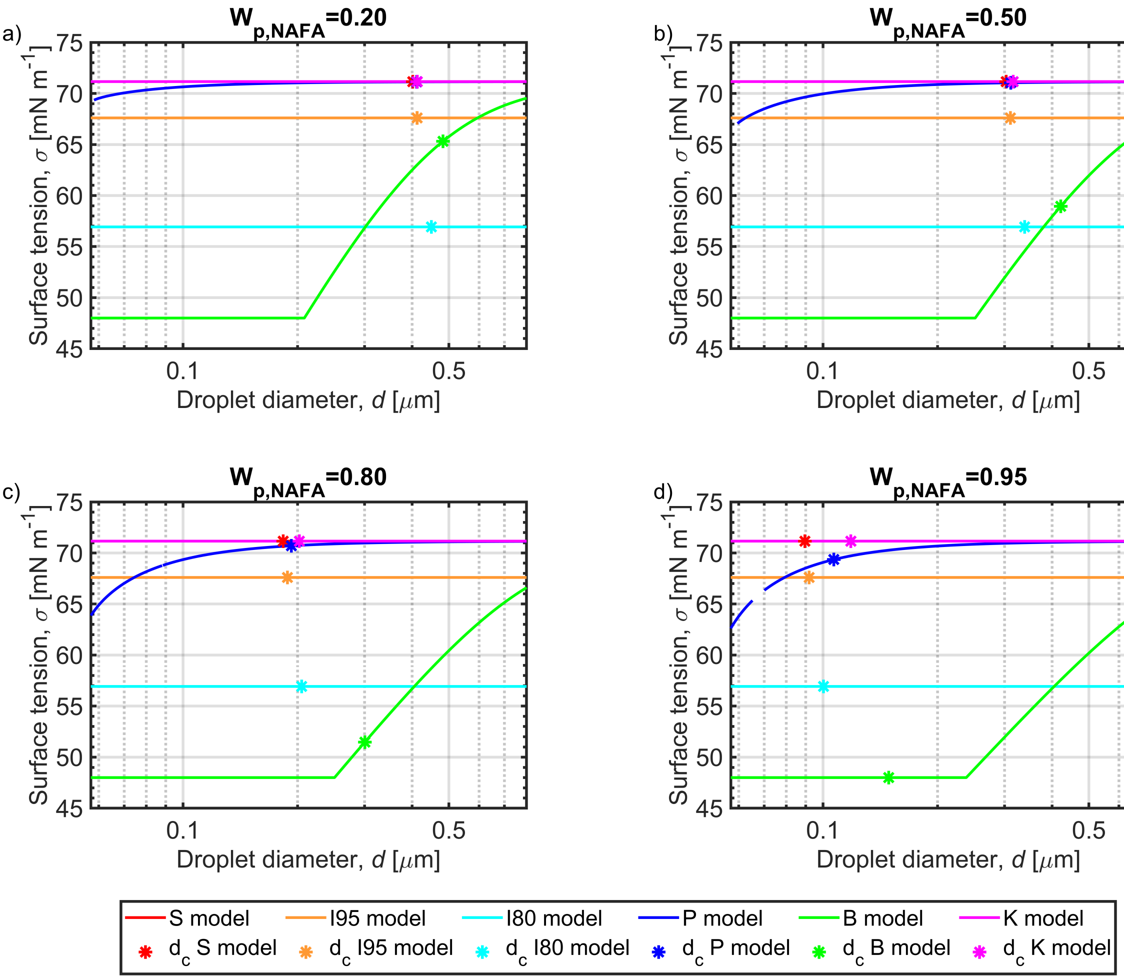

Figure 5. Surface tension along Köhler curves for growing aqueous NAFA–NaCl droplets formed from 50 nm dry particles with NAFA mass fractions of (a) 0.20, (b) 0.50, (c) 0.80, and (d) 0.95, calculated with the different models described in Section 2.3. The critical points of droplet activation (SS_c) presented in Figs. 1 and S3 are indicated with asterisks on each surface tension curve.

in activating droplets predicted with a thermodynamic partitioning model based on similar Szyszkowski-type surface tension and Gibbs adsorption equations as used for the present mass-based framework (Prisle et al., 2008, 2010, 2011). As the simple partitioning model (S) was developed to specifically describe properties of droplets at the critical point of activation, it was not *a priori* expected that conditions of vanishing surface tension and water activity reduction would be realized throughout droplet growth and activation, in particular not at the earlier stages along the Köhler curve. However, the smaller the droplet, the larger the A/V and resulting surface/bulk partitioning (surface enhancement) factor, and except for the earliest stages of droplet growth where overall droplet concentrations are the highest, droplet bulk concentrations are nearly completely depleted by surface adsorption. Therefore, in the case of NAFA particles, as for the simple, strong surfactants SDS and fatty acid salts, conditions described with the thermodynamic partitioning model (P) are closely represented by the simple partitioning model (S) for a range of droplet sizes, including the critical point of activation.

In a macroscopic solution, a strong surfactant which is fully partitioned to the surface would be expected to signaficantly reduce solution surface tension and the situation described by model (S) would be quite unrealistic. However, Köhler model predictions with the insoluble surfactant representation (I), where NAFA has no impact on droplet water activity and surface tension is moderately reduced, do not represent either the CCN data of Kristensen et al. (2014) or the full partitioning model predictions, well and the agreement decreases when surface tension is further decreased (therefore not included here). Specifically, insoluble surfactant representation fails to reproduce the variation of CCN activity with dry particle mixing state, and therefore the composition-dependent balance between Kelvin and Raoult terms. Is is however entirely possible that the properties described by representation (I) could provide good agreement with both experimental data and the full model (P) in cases of less surface active aerosol mixtures, which are less strongly surface adsorbed and depleted from the droplet bulk.

Similar mechanisms as predicted with the thermodynamic partitioning model for activation of NAFA particles in this work could be present for the bacterial biopolymers investigated by Dawson et al. (2016) as proxy for complex marine hydrogels. These substances produce significant surface tension reduction in macroscopic solutions, which is not reflected in experimental hygroscopic properties for aerosol mixtures with various salts. Dawson et al. (2016) provide crosslinking between polymers and formation of insoluble complexes as possible explanations. Another mechanism could be bulk depletion from surface partitioning, which was predicted to impact the Köhler curves for NAFA particles also at much earlier stages than the critical point of activation.

The very poor performance of model (B) with respect to both CCN data from Kristensen et al. (2014) and predictions of the thermodynamic partitioning model (P), in contrast to the good performance of (S), shows that for the studied NAFA–NaCl mixtures, the most significant impact of surface activity on cloud microphysics is on bulk-phase depletion from surface partitioning, and notably *not* on surface tension reduction in activating droplets. Calculations with model (P) use the same composition-dependent surface tension and water activity relations as model (B), based on measurements made for macroscopic solutions (Eqs. 8 and 11). Several previous studies have highlighted that application of macroscopic relations without correcting the droplet bulk composition for depletion of surface active components from bulk/surface partitioning onto the large droplet surfaces fails to reproduce experimentally observed CCN activity for a variety of surface active organic aerosol (Prisle et al., 2008, 2010, 2011; Petters and Petters, 2016; Forestieri et al., 2018; Lin et al., 2018). When macroscopic composition-dependent relations for surface tension, as well as other solution properties, are connected to microscopic droplet states *via* a bulk/surface partitioning model, the effect of bulk/surface partitioning in droplets is to move the solution mixing state to a different point in the composition domain, as illustrated in Figs. 2 and 3 for the present case of NAFA–NaCl droplet mixtures.

Including surface tension effects of surface active aerosol components without considering the altered bulk-phase composition from surface partitioning will lead to greater errors in estimating CCN activity than neglecting surface activity altogether: The basic Köhler model (K) which disregards all effects pertaining to NAFA surface activity is able to capture both measured CCN activity of the mixed NAFA–NaCl particles and Köhler predictions with model (P) surprisingly well, even if NAFA indeed shows significant surfactant strength in macroscopic aqueous solutions. Similar conclusions were made in previous studies for particle mixtures of strong, simple surfactants SDS and fatty acid salts with NaCl (Sorjamaa et al., 2004; Prisle et al., 2008, 2010; Forestieri et al., 2018). Detailed analysis showed that the good agreement of the basic Köhler model with measured CCN activity and close resemblance to predictions from the comprehensive partitioning model are in large part due to cancellation effects between the perturbations in predicted Kelvin (surface tension depression) and Raoult (water activity depression) terms of the Köhler curves, introduced by a full account of surface activity, compared to the basic Köhler model (Prisle et al., 2008, 2010). Here, we see the same cancellation between differences in the critical Kelvin and Raoult terms for NAFA–NaCl particles, when comparing predictions from models (K) and (P). Evident as a close similarity between the basic Köhler and comprehensive partitioning model predictions, as well as experiments, this may prove to be a signature feature of CCN activity for relatively strong surfactants, in particular for compounds and mixtures with large $\bar{M}_i$, including macromolecules such as model-HULIS and biopolymers (Dawson et al., 2016).

This nearly full cancellation of surface activity effects on Kelvin and Raoult terms may not be present in droplet activation for all types of surface active aerosol components and mixtures. Which general features of these systems are driving the impact of surface activity in cloud microphysics remains to firmly established *via* predictive, thermodynamically consistent Köhler modeling using independently derived mixture-specific model parameters.

3.4.1 Other surface partitioning models

Several bulk/surface partitioning models have been presented and deployed in Köhler calculations to reproduce measured CCN activity for surface active aerosol systems with varying degrees of success. Common for these models is that macroscopic solution property–composition relations are connected to those of a growing droplet with changing A/V based on an adsorption isotherm and surface tension equation of state for the surface active components. As in the present work, Gibbsian adsorption with Szyszkowski-type surface tension equations have been most widely used, however, to our knowledge, this is the first time such a comprehensive, predictive Gibbsian bulk/surface partitioning framework has been applied on a mass-basis, allowing for thermodynamically consistent Köhler modeling of complex, chemically unresolved surface active aerosol. The advantage of the present model is that it is fully predictive and take all non-ideal interactions into account via continuous parametrizations independently constrained by measurements. No additional parameters are introduced in the framework. A remaining disadvantage is that while water activity and surface tension can be accurately measured with standard instrumentation, these experiments and the construction of suitable multi-dimensional parametrizations are still non-trivial and require significant amounts of sample material to obtain a sufficient number of data points for robust fits.

The model presented by Ruehl et al. (2016) is in the "gaseous film" region essentially the same as the simple partitioning model (S) by Prisle et al. (2011). All surface active material is partitioned to the droplet surface, but the total amount is still less than what is necessary to reach a minimum surface concentration, expressed *via* the δ_{org} parameter (interpreted as a minimum surface thickness), that enables full surface coverage and reduced surface tension. Ruehl et al. (2016) found that droplet activation typically occurs in this gaseous film surface regime, analogously to the observations of the present work and Prisle et al. (2010, 2011) for the full Gibbsian partitioning model and simple model (S). Köhler calculations with the full partitioning model however show that activation does not always occur exactly at the point where surface tension reaches that of water (δ_{org}, point of film rupture in Ruehl's model). Prior to activation, the Ruehl et al. (2016) model accounts for concentration-dependent reduced surface tensions of the investigated droplet systems. Using a surface-composition based surface tension equation, they find a quite different surface tension dependency on droplet size, than seen with the Szyszkowski-type equation in this work. However, their study also involves surface active aerosols with quite different characteristics, compared to the NAFA mixtures studied here. They furthermore do not seem to include effects of non-ideal solute interactions on growing droplet water activity, which could also lead to differences compared to the present work. The model of Ruehl et al. (2016) is first fitted to the droplet size–relative humidity data being described, in order to obtain the necessary surface tension and adsorption parameters. As such, their model is analytical, rather than predictive, and could not be fitted to the CCN data for supersaturated conditions used to validate model prediction of this work. In the present work, both surface tension and water activity parameters are obtained independently of the predicted CCN measurements by fitting to (marcoscopic) composition-dependent data.

The simple "complete phase-separation" model of Ovadnevaite et al. (2017) also assumes that surface active components are fully partitioned to the droplet surface, similar to the model of Prisle et al. (2011) and the gaseous film model of Ruehl et al. (2016). The detailed liquid-liquid phase separation (LLPS) model of Ovadnevaite et al. (2017) describes the composition-dependent partitioning equilibrium between an aqueous (bulk) and organic (surface) phase of a droplet. Contrary to the full partitioning model (P) of the present work, and the "compressed film" model of Ruehl et al. (2016), which both consider the surface to be comprised exclusively of the surface active material, the LLPS model of Ovadnevaite et al. (2017) accounts for presence of small amounts of organic in the aqueous phase, as well as water and water-soluble components in the organic phase. They evaluate droplet surface tensions from an empirical mixing rule, based on the mass-weighed composition of the phase-separated organic (surface) phase. Effects of solution non-ideality in the aqueous phase are considered using the well-established AIOMFAC model. Their predictive calculations are enabled by assuming a well-defined proxy mixture to represent the surface active aerosol component, with the inherent uncertainties related to the choice of proxy system and variation of solute-solvent and solute-solute interaction parameters across droplet composition space. The proxy mixture used by Ovadnevaite et al. (2017) appears to be less surface active than the NAFA system studied here. In the Gibbsian–Szyszkowski partitioning representation (P), this would entail less strong depletion of the surface active component from the droplet bulk phase due to surface adsorption and thus higher likelihood of (moderately) reduced droplet surface tension, including at the point of droplet activation. The particles representing so-called nascent ultrafine mode (NUM) events observed by Ovadnevaite et al. (2017) are of similar sizes as some of the smallest particle sizes studied in the present work, which activate for smaller growth factors, corresponding to more concentrated solutions, where surface tension is indeed more likely to be reduced in the absence of strong bulk depletion effects from surface adsorption.

Similarly to the Ovadnevaite et al. (2017) LLPS model, the monolayer partitioning model of Malila and Prisle (2018) allows for partitioning of all droplet components between both bulk and surface phases. The partitioning occurs according to a semi-empirical mixing rule to yield surface-composition dependent solution surface tension matching the surface tension evaluated for the corresponding bulk-composition. Instead of assuming a proxy solution mixture as for the LLPS model, effects of non-ideality on surface adsorption are accounted for by using experimentally-based composition-dependent solution properties.

By using mass-based relations and assuming an average volume of the partitioning unit (Lin et al., 2018) analogously to the approach of the present work, this allows for applications to chemically unresolved surface active mixtures without explicitly defining all specific interactions between solution components. The monolayer model of Malila and Prisle (2018) provides an alternative to the Gibbsian models for performing predictive Köhler predictions of droplet growth and activation with independently determined interaction parameters for both well-known and unresolved droplet mixtures. The monolayer model has been found to predict lower droplet surface tensions than the Gibbsian models, because the surface partitioning factor $m^S_{\mathrm{sft}}/m^B_{\mathrm{sft}}$ is restricted to a finite value by the volume of the surface monolayer, leading to less strong depletion of the droplet bulk (Malila and Prisle, 2018; Lin et al., 2018, 2020; Bzdek et al., 2020).

It is occasionally questioned whether partitioning models are valid at all for CCN measurements, due to the long equilibration times of (macroscopic) surface tension (Fainerman et al., 2002; Noziere et al., 2014; Van den Bogaert and Joos, 1979, 1980; Wen et al., 1998; Coltharp and Franses, 1996) compared to particle and droplet residence times in commonly used cloud condensation nucleus counters (Prisle et al., 2008; Kristensen et al., 2014). Lin et al. (2020) presented a detailed analysis of the effects of using surface tension parametrizations corresponding to different measurement times in Köhler calculations. They observe complex relations between the influence of droplet size and composition, surface adsorption, and measurement time. A clear progression of predicted surface adsorption in droplets is seen when using surface tension parametrizations corresponding to successively longer measurement times, but the effects of this surface adsorption on the individual Kelvin and Raoult terms of the droplet growth curve nearly cancel at every time step. We are currently not aware of any experiment that would allow verification of these predictions and only of this single existing data set to enable similar calculations with considerations of time dependence in connection with bulk/surface partitioning, therefore the general nature of these phenomena is currently unclear.

3.4.2 Large-scale applications

Thermodynamically consistent, predictive partitioning models enable investigating details about how droplet properties change under the impact of surface activity as they grow and activate. However, the double iterative scheme employed in the comprehensive model (P) is computationally not feasible for applications to large-scale simulations (Prisle et al., 2012) Representation (K) is computationally much simpler to use than the comprehensive partitioning model (P) and has thus been favored over the latter for calculations of CCN activity, in light of the ambiguity of performance of the two models with respect to data as well as in global simulations (Prisle et al., 2012). However, the simple representation (S) is equally easy to implement in a large-scale framework (Prisle et al., 2011, 2012) and has the additional advantage that contributions of the surface active components to both hygroscopicity and surface tension are known without specific knowledge of the composition of the particle mixtures. These features make (S) applicable to larger scale modelling of CCN activation for real atmospheric aerosols (Prisle et al., 2011, 2012). The good performance of (S) with respect to both data and comprehensive calculations for mixed NAFA–NaCl particles renders the simple representation as a promising candidate for representing effects of strong surface activity on CCN potential of other complex and unresolved organic aerosol mixtures.

4 Conclusions

We present a framework for including bulk/surface partitioning of chemically unresolved surface active components in Köhler modeling of growing droplets, using mass-based Gibbs adsorption and Szyszkowski surface tension equations. The comprehensive framework (P) was applied to calculate CCN activity for particles comprising chemically unresolved NAFA in mixtures with NaCl. Continuous, ternary parametrizations of surface tension and water activity as functions of both NAFA and NaCl aqueous mass concentrations, as required input for the model, were constructed from measurements. Comprehensive, thermodynamically consistent predictions were used to benchmark four alternative representations of the effect of NAFA surface activity in cloud droplet activation: (S) the simple partitioning representation proposed by Prisle et al. (2011), where NAFA is assumed to have zero intrinsic influence on both surface tension and water activity of droplets, (I) considering NAFA as a fully surface-partitioned, insoluble surfactant with fixed surface tension reduction, (B) assuming that droplets comprising NAFA and NaCl have identical properties to macroscopic bulk solutions of the same overall composition, and (K) treating NAFA and NaCl alike as regular soluble and homogeneouly distributed (non-surface active) solutes.

Results of our calculations show that assuming macroscopic solution properties for activating droplets in the micron and sub-micron size range lead to gross overestimations of measured CCN activity, whereas other frameworks including bulk-surface partitioning and/or omitting surface tension reduction each describe the previously reported CCN data for NAFA–NaCl particles well. These latter models give mutually similar results for both critical supersaturations, as well as a number of other properties calculated for activating droplets. NAFA has significant surfactant strength in macroscopic aqueous solutions, but due to the very large surface-to-volume ratios of sub-micron activating droplets, the NAFA partitioning equilibrium is strongly shifted toward the surface and the same total compositions do not lead to similar, if any, reductions in droplet surface tension as in macroscopic solutions. NAFA has only modest influence on water activity in both macroscopic aqueous solutions and activating droplets alike, at least in part due to its high average molar mass, compared to hygroscopic salts. In sub-micron droplets, the weak intrinsic impact on water activity is further dampened by surface partitioning of NAFA.

With experimentally constrained accounts of non-ideal interactions in both water activity and NAFA surface activity, we therefore predict cloud microphysical behavior for chemically complex aerosol mixtures which closely resembles that previously seen for systems comprising simple, strong surfactants with well-defined molecular properties. Sub-micron droplet properties are governed by size-modulated influences of surface activity on both water activity and curvature terms of the Köhler curve and the "missing Raoult effect" from bulk-phase depletion due to surface adsorption overpowers any enhancement of droplet growth and activation from decreased surface tension. We are currently not aware of any other chemically unresolved or complex aerosol system for which experimental data are available to enable a similar analysis. However, we hope that the presented framework will motivate more measurements to provide thermodynamically consistent characterization for a broad range of surface active aerosol systems. This will contribute significantly to clarify the compositions and conditions where each of the effects of aerosol surface activity is dominating cloud microphysics. From the early demonstrations of reduced surface tension of atmospheric cloud water to the remaining diverging observations for surface tension effects in cloud microphysics, the present results underscore that organic surface activity may be one of the key features to constrain for the understanding and modeling of aerosol–cloud–climate interactions (Prisle et al., 2012; Lowe et al., 2019).

Finally, surface activity of aerosol components may have important implications for other atmospheric processes in addition to cloud microphysics, including heterogeneous chemistry on aqueous droplet surfaces. Owing to the large surface areas, aqueous surface chemistry may be significantly enhanced on submicron droplets. One example is the photosensitized limonene uptake by Humic Acid, another atmospheric model HULIS, recently described by Tsui and McNeill (2018). A comprehensive description of droplet surface composition, including size-dependent surface adsorption and response to changing ambient humidity and droplet growth, may be crucial for understanding and predicting the extent of such processes.

Author contributions. NLP conceived, planned and secured funding for the project. BM made the surface tension and water activity parametrizations supervised by NLP. NLP did the model implementation and made the model calculations, analyzed all results, and wrote the first and revised versions of the manuscript and the response to reviewers.

Competing interests. The authors declare no competing interests.

Acknowledgements. The authors thank Silvia Calderón, Jack J. Lin, Jussi Malila, Tomi Raatikainen, and Taina Yli-Juuti for comments and technical support, and Thomas B. Kristensen and Merete Bilde for providing measurement data previously published by Kristensen et al. (2014) and Lin et al. (2020). This project has received funding from the European Research Council (ERC) under the European Union's Horizon 2020 research and innovation programme (Project SURFACE, Grant Agreement No. 717022). N. L. Prisle also gratefully acknowledges funding from the Carlsberg Foundation (Grants 2009_01_0366 and 2010_01_0391) and Academy of Finland (Grants 257411, 314175, and 308238).

References

Asa-Awuku, A., Sullivan, A., Hennigan, C. J., Weber, R. J., and Nenes., A.: Investigation of molar volume and surfactant characteristics of water-soluble organic compounds in biomass burning aerosol, Atmospheric Chemistry and Physics, 8, 799–812, 2008.

Aumann, E., Hildemann, L., and Tabazadeh, A.: Measuring and modeling the composition and temperature-dependence of surface tension for organic solutions, Atmospheric Environment, 44, 329–337, 1967.

Bianco, H. and Marmur, A.: The Dependence of the Surface Tension of Surfactant Solutions on Drop Size, Journal of Colloid and Interface Science, 151, 517–522, 1992.

Bilde, M. and Svenningsson, B.: CCN Activation of Slightly Soluble Organics: The Importance of Small Amounts of Inorganic Salt and Particle Phase, Tellus, 56B, 128–134, 2004.

Booth, A. M., Topping, D. O., McFiggans, G., and Percival, C. J.: Surface tension of mixed inorganic and dicarboxylic acid aqueous solutions at 298.15 K and their importance for cloud activation predictions, Phys. Chem. Chem. Phys., 11, 8021–8028, 2009.

Bzdek, B. R., Reid, J. P., Malila, J., and Prisle, N. L.: The surface tension of surfactant-containing, finite volume droplets, Proceedings of the National Academy of Sciences, 117, 8335–8343, 2020.

Cheng, Y., Li, S.-M., Leithead, A., Brickell, P. C., and Leaitch, W. R.: Characterizations of *cis*-pinonic acid and n-fatty acids on fine aerosols in the Lower Fraser Valley during Pacific 2001 Air Quality Study, Atmospheric Environment, 38, 5789–5800, 2004.

Coltharp, K. A. and Franses, E. I.: Equilibrium and dynamic surface tension behavior of aqueous soaps: sodium octanoate and sodium dodecanoate (sodium laurate), Colloids and Surfaces A: Physicochemical and Engineering Aspects, 108, 225–242, 1996.

Dawson, K. W., Petters, M. D., Meskhidze, N., Suda Petters, S., and Kreidenweis, S. M.: Hygroscopic growth and cloud droplet activation of xanthan gum as a proxy for marine hydrogels, Journal of Geophysical Research: Atmospheres, 121, 11 803–11 818, 2016.

Dillmann, A. and Meier, G. E. A.: A refined droplet approach to the problem of homogeneous nucleation from the vapor phase, The Journal of Chemical Physics, 94, 3872–3884, https://doi.org/10.1063/1.460663, https://doi.org/10.1063/1.460663, 1991.

Dinar, E., Mentel, T. F., and Rudich, Y.: The density of humic acids and humic like substances (HULIS) from fresh and aged wood burning and pollution aerosol particles, Atmospheric Chemistry and Physics, 6, 5213–5224, 2006a.

Dinar, E., Taraniuk, I., Graber, E. R., Katsman, S., Moise, T., Anttila, T., Mentel, T. F., and Rudich, Y.: Cloud Condensation Nuclei properties of model and atmospheric HULIS, Atmospheric Chemistry and Physics, 6, 2465–2481, 2006b.

Facchini, M., Mircea, M., Fuzzi, S., and Charlson, R.: Cloud Albedo Enhancement by Surface-Active Organic Solutes in Growing Droplets, Nature, 401, 257–259, https://doi.org/10.5194/acp-10-8219-2010, 1999.

Facchini, M., Decesari, S., Mircea, M., Fuzzi, S., and Loglio, G.: Surface Tension of Atmospheric Wet Aerosol and Cloud/Fog Droplets in Relation to their Organic Carbon Content and Chemical Composition, Atmospheric Environment, 34, 4853–4857, 2000.

Fainerman, V. B., Miller, R., and Möhwald, H.: General Relationships of the Adsorption Behavior of Surfactants at the Water/Air Interface, J. Phys. Chem. B, 106, 809–819, 2002.

Forestieri, S. D., Staudt, S. M., Kuborn, T. M., Faber, K., Ruehl, C. R., Bertram, T. H., and Cappa, C. D.: Establishing the impact of model surfactants on cloud condensation nuclei activity of sea spray aerosol mimics, Atmospheric Chemistry and Physics, 18, 10 985–11 005, 2018.

Frosch, M., Prisle, N. L., Bilde, M., Varga, Z., and Kiss, G.: Joint effect of organic acids and inorganic salts on cloud droplet activation, Atmospheric Chemistry and Physics, 11, 3895–3911, https://doi.org/10.5194/acp-11-3895-2011, 2011.

Gérard, V., Nozière, B., Baduel, C., Fine, L., Frossard, A. A., and Cohen, R. C.: Anionic, Cationic, and Nonionic Surfactants in Atmospheric Aerosols from the Baltic Coast at Askö, Sweden: Implications for Cloud Droplet Activation, Environmental Science & Technology, 50, 2974–2982, 2016.

Gibbs, J., Bumstead, H., Longley, W., and Name, R. V.: The Collected Works of J. Willard Gibbs, Longmans, Green and Co., 1928.

Graber, E. R. and Rudich, Y.: Atmospheric HULIS: How humic-like are they? A comprehensive and critical review, Atmos. Chem. Phys., 6, 729–753, 2006.

Hansen, A. M. K., Hong, J., Raatikainen, T., Kristensen, K., Ylisirniö, A., Virtanen, A., Petäjä, T., Glasius, M., and Prisle, N. L.: Hygroscopic properties and cloud condensation nuclei activation of limonene-derived organosulfates and their mixtures with ammonium sulfate, Atmospheric Chemistry and Physics, 15, 14 071–14 089, https://doi.org/10.5194/acp-15-14071-2015, http://www.atmos-chem-phys.net/15/14071/2015/, 2015.

Harmon, C., Grimm, R., McIntire, T., Peterson, M., Njegic, B., Angel, V., Alshawa, A., Underwood, J., Tobias, D., Gerber, R., Gordon, M., Hemminger, J., and Nizkorodov, S.: Hygroscopic growth and deliquescence of NaCl nanoparticles mixed with surfactant SDS, Journal of Physical Chemistry B, 114, 2435–2449, 2010.

Hyvärinen, A.-P., Lihavainen, H., Gaman, A., Vairila, L., Ojala, H., Kulmala, M., and Viisanen, Y.: Surface Tensions and Densities of Oxalic, Malonic, Succinic, Maleic, Malic, and *cis*-Pinonic Acids, Journal of Chemical and Engineering Data, 51, 255–260, 2006.

Kiss, G., Tombacz, E., and Hansson, H.-C.: Surface Tension Effects of Humic-Like Substances in the Aqueous Extract of Tropospheric Fine Aerosol, Journal of Atmospheric Chemistry, 50, 279–294, 2005.

Köhler, H.: The Nucleus in and the Growth of Hygroscopic Droplets, Transactions of the Faraday Society, 32, 1152–1161, 1936.

Kristensen, T. B., Prisle, N. L., and Bilde, M.: Cloud droplet activation of mixed model HULIS and NaCl particles: Experimental results and κ-Köhler theory, Atmospheric Research, 137, 167–175, 2014.

Kroflič, A., Frka, S., Simmel, M., Wex, H., and Grgić, I.: Size-resolved surface active substances of atmospheric aerosol: reconsideration of the impact on cloud droplet formation, Environmental Science & Technology, 0, null, https://doi.org/10.1021/acs.est.8b02381, https://doi.org/10.1021/acs.est.8b02381, pMID: 30048123, 2018.

Laaksonen, A.: The Composition Size Dependence of Aerosols Created by Dispersion of Surfactant Solutions, Journal of Colloid and Interface Science, 159, 517–519, 1993.

Li, Z., Williams, A., and Rood, M.: Influence of Soluble Surfactant Properties on the Activation of Aerosol Particles Containing Inorganic Solute, Journal of the Atmospheric Sciences, 55, 1859–1866, 1998.

Lin, J. J., Malila, J., and Prisle, N. L.: Cloud droplet activation of organic–salt mixtures predicted from two model treatments of the droplet surface, Environmental Science: Processes & Impacts, 20, 1611–1629, 2018.

Lin, J. J., Kristensen, T. B., Calderón, S. M., Malila, J., and Prisle, N. L.: Effects of surface tension time-evolution for CCN activation of a complex organic surfactant, Environmental Science: Processes & Impacts, 22, 271–284, 2020.

Low, R.: A Theoretical Study of Nineteen Condensation Nuclei, Journal de Recherches Atmospheriques, pp. 65–78, 1969.

Lowe, S. J., Partridge, D. G., Davies, J. F., Wilson, K. R., Topping, D., and Riipinen, I.: Key drivers of cloud response to surface-active organics, Nature Communications, 10, 1–12, 2019.

Mäkelä, J. and Manninen, P.: Molecular size distribution od structure investigations of humic substances in groundwater, working report 2008-36, Posiva Oy, Posiva Oy, Olkiluoto, FI-27160 Eurajoki, Finland, 2008.

Malila, J. and Prisle, N. L.: A monolayer partitioning scheme for droplets of surfactant solutions, Journal of Advances in Modeling Earth Systems, 10, 3233–3251, 2018.

Meissner, H. P. and Michaels, A. S.: Surface Tensions of Pure Liquids and Liquid Mixtures, Industrial & Engineering Chemistry, 41, 2782–2787, https://doi.org/10.1021/ie50480a028, https://doi.org/10.1021/ie50480a028, 1949.

Mochida, M., Kitamori, Y., Kawamura, K., Nojiri, Y., and Suzuki, K.: Fatty acids in the marine atmosphere: Factors governing their concentrations and evaluation of organic films on sea-salt particles, Journal of Geophysical Research, 107, D17S4325, https://doi.org/10.1029/2001JD001278, 2002.

Mochida, M., Kawamura, K., Umemoto, N., Kobayashi, M., Matsunaga, S., Lim, H.-J., Turpin, B., Bates, T., and Simoneit, B.: Spatial distributions of oxygenated organic compounds (dicarboxylic acids, fatty acids, and levoglucosan) in marine aerosols over the western Pacific and off the coast of East Asia: Continental outflow of organic aerosols during the ACE-Asia campaign, Journal of Geophysical Research, 108, D23S8638, https://doi.org/10.1029/2002JD003249, 2003.

Noziere, B., Baduel, C., and Jaffrezo, J.-L.: The dynamic surface tension of atmospheric aerosol surfactants reveals new aspectsof cloud activation, Nature Communications, 5, 1–7, 2014.

Ovadnevaite, J., Zuend, A., Laaksonen, A., Sanchez, K. J., Roberts, G., Ceburnis, D., Decesari, S., Rinaldi, M., Hodas, N., Facchini, M. C., Seinfeld, J. H., and O' Dowd, C.: Surface tension prevails over solute effect in organic-influenced cloud droplet activation, Nature, 546, 637–641, 2017.

Petters, M. and Kreidenweis, S.: A single parameter representation of hygroscopic growth and cloud condensation nucleus activity–Part 3: Including surfactant partitioning, Atmos. Chem. Phys., 13, 1081–1091, 2013.

Petters, M. D. and Kreidenweis, S. M.: A single parameter representation of hygroscopic growth and cloud condensation nucleus activity, Atmos. Chem. Phys., 7, 1961–1971, 2007.

Petters, S. S. and Petters, M. D.: Surfactant effect on cloud condensation nuclei for two-component internally mixed aerosols, Journal of Geophysical Research: Atmospheres, 121, 2016.

Poulain, L., Wu, Z., Petters, M. D., Wex, H., Hallbauer, E., Wehner, B., Massling, A., Kreidenweis, S. M., and Stratmann, F.: Towards closing the gap between hygroscopic growth and CCN activation for secondary organic aerosols - Part 3: Influence of the chemical composition on the hygroscopic properties and volatile fractions of aerosols, Atmos. Chem. Phys., 10, 3775–3785, 2010.

Prisle, N.: Cloud Condensation Nuclei Properties of Organic Aerosol Particles: Effects of Acid Dissociation and Surfactant Partitioning, M.Sc. Thesis, Department of Chemistry, Faculty of Science, University of Copenhagen, 2006.

Prisle, N. L., Raatikainen, T., Sorjamaa, R., Svenningsson, B., Laaksonen, A., and Bilde, M.: Surfactant partitioning in cloud droplet activation: a study of C8, C10, C12 and C14 normal fatty acid sodium salts, Tellus, 60B, 416–431, https://doi.org/10.1111/j.1600-0889.2008.00352.x, 2008.

Prisle, N. L., Raatikainen, T., Laaksonen, A., and Bilde, M.: Surfactants in cloud droplet activation: mixed organic-inorganic particles, Atmos. Chem. Phys., 10, 5663–5683, https://doi.org/10.5194/acp-10-5663-2010, 2010.

Prisle, N. L., Dal Maso, M., and Kokkola, H.: A simple representation of surface active organic aerosol in cloud droplet formation., Atmos. Chem. Phys., 11, 4073–4083, https://doi.org/10.5194/acp-11-4073-2011, 2011.

Prisle, N. L., Asmi, A., Topping, D., Partanen, A.-I., Romakkaniemi, S., Dal Maso, M., Kulmala, M., Laaksonen, A., Lehtinen, K. E. J., McFiggans, G., and Kokkola, H.: Surfactant effects in global simulations of cloud droplet activation., Geophys. Res. Lett., 39, L05 802, https://doi.org/10.1029/2011GL050467, 2012.

Prisle, N. L., Lin, J. J., Purdue, S., Lin, H., Meredith, J. C., and Nenes, A.: Cloud condensation nuclei activity of six pollenkitts and the influence of their surface activity, Atmospheric Chemistry and Physics, 19, 4741–4761, 2019.

Raatikainen, T. and Laaksonen, A.: A simplified treatment of surfactant effects on cloud drop activation, Geosci. Model Dev., 4, 107–116, https://doi.org/10.5194/gmd-4-107-2011, 2011.

Rood, M. J. and Williams, A. L.: Reply, Journal of the Atmospheric Sciences, 58, 1468–1473, 2001.

Ruehl, C. R., Chuang, P. Y., and Nenes, A.: Aerosol hygroscopicity at high (99 to 1001329–1344, https://doi.org/10.5194/acp-10-1329-2010, http://www.atmos-chem-phys.net/10/1329/2010/, 2010.

Ruehl, C. R., Davies, J. F., and Wilson, K. R.: An interfacial mechanism for cloud droplet formation on organic aerosols, Science, 351, 1447–1450, https://doi.org/10.1126/science.aad4889, http://science.sciencemag.org/content/351/6280/1447, 2016.

Shulman, M., Jacobson, M., Charlson, R., Synovec, R., and Young, T.: Dissolution Behavior and Surface Tension Effects of Organic Compounds in Nucleating Cloud Droplets, Geophysical Research Letters, 23, 277–280, 1996.

Sorjamaa, R., Svenningsson, B., Raatikainen, T., Henning, S., Bilde, M., and Laaksonen, A.: The Role of Surfactants in Köhler Theory Reconsidered, Atmospheric Chemistry and Physics, 4, 2107–2117, 2004.

Topping, D.: An analytical solution to calculate bulk mole fractions for any number of components in aerosol droplets after considering partitioning to a surface layer, Geoscientific Model Development, 3, 635–642, https://doi.org/10.5194/gmd-3-635-2010, http://www.geosci-model-dev.net/3/635/2010/, 2010.

Tsui, W. G. and McNeill, V. F.: Modeling Secondary Organic Aerosol Production from Photosensitized Humic-like Substances (HULIS), Environmental Science & Technology Letters, 5, 255–259, https://doi.org/10.1021/acs.estlett.8b00101, https://doi.org/10.1021/acs.estlett.8b00101, 2018.

Van den Bogaert, R. and Joos, P.: Dynamic surface tensions of sodium myristate solutions, The Journal of Physical Chemistry, 83, 2244–2248, 1979.

Van den Bogaert, R. and Joos, P.: Diffusion-controlled adsorption kinetics for a mixture of surface active agents at the solution-air interface, The Journal of Physical Chemistry, 84, 190–194, 1980.

Vanhanen, J., Hyvärinen, A.-P., Anttila, T., Raatikainen, T., Viisanen, Y., and Lihavainen, H.: Ternary solution of sodium chloride, succinic acid and water; surface tension and its influence on cloud droplet activation, Atmospheric Chemistry and Physics, 8, 4595–4604, 2008.

Varga, Z., Kiss, G., and Hansson, H.-C.: Modelling the cloud condensation nucleus activity of organic acids on the basis of surface tension and osmolality measurements, Atmospheric Chemistry and Physics, 7, 4601–4611, 2007.

Wen, X. Y., McGinnis, K. C., and Franses, E. I.: Unusually low dynamic surface tensions of aqueous solutions of sodium myristate, Colloids and Surfaces A: Physicochemical and Engineering Aspects, 143, 371–380, 1998.

Wex, H., Hennig, T., Salma, I., Ocskay, R., Kiselev, A., Henning, S., Massling, A., Wiedensohler, A., and Stratmann, F.: Hygroscopic growth and measured and modeled critical supersaturations of an atmospheric HULIS sample, GEOPHYSICAL RESEARCH LETTERS, 34, L02 818, https://doi.org/10.1029/2006GL028260, 2007.

Yassaa, N., Meklati, B. Y., Cecinato, A., and Marino, F.: Particulate n-alkanes, n-alkanoic acids and polycyclic aromatic hydrocarbons in the atmosphere of Algiers City Area, Atmospheric Environment, 35, 1843–1851, 2001.

Zamora, I. R. and Jacobson, M. Z.: Measuring and modeling the hygroscopic growth of two humic substances in mixed aerosol particles of atmospheric relevance, Atmos. Chem. Phys., 13, 8973–8989, https://doi.org/10.5194/acp-13-8973-2013, 2013.